Reply to reviews on the manuscript
Modal sensitivity of rock glaciers to elastic changes from spectral seismic noise monitoring and modeling

By Antoine Guillemot, Laurent Baillet, Stéphane Garambois, Xavier Bodin, Agnès Helmstetter, Raphaël Mayoraz, Eric Larose

Contact :
Antoine GUILLEMOT
ISTerre, Université Grenoble Alpes
Grenoble (France)
antoine.guillemot@univ-grenoble-alpes.fr

Dear reviewer, dear editor,

We would like to thank you for the constructive review following the submission of our manuscript "***Modal sensitivity of rock glaciers to elastic changes from spectral seismic noise monitoring and modeling***" to *The Cryosphere*. We took into account all the comments from the two reviewers and editor.

One of the main problems raised concerns the lack of references to the HSVR method. Indeed, we didn't specified clearly that our seismometers are single (vertical) component, so that the HSVR method was inapplicable in our case. However, we added some mentions to previous publications on this method successfully applied on permafrost, since the methodology is very similar to spectral analysis presented in this article.

Furthermore, you suggested additional figures to demonstrate the feasibility of our method: one showing the temporal evolution of modeled resonance frequencies, and another one showing modeled amplitude of the spectrum for a particular state of freezing. Unfortunately, both of them are difficult to address accurately to our mind, because of the lack of information concerning thermo-mechanical coupling and 3D effects on the rock glaciers. We detail these points further in our response.

As suggested by the reviewers, we also modified some sentences and figures in order to improve both the quality of information that we provide and the readability of the publication. We added also some references to publications about seismic monitoring on permafrost and glaciers, as a completed state of art.

Please find below a point-by-point response to all your major comments (our answers in red), in complement to the new manuscript with highlighted main changes (text in red as well).

Sincerely yours,

On behalf of the authors,

Antoine Guillemot

Comments reviewer 1 (Andreas Kohler)

This is a very good and comprehensive study demonstrating the ability of passive seismic measurements for time-lapse monitoring of near-surface structures in combination with other geophysical methods which provide more high-resolution, but time-restricted information. The presented use of modal analysis in particular is a novel and promising approach for rock glacier monitoring. The results presented in this study support the capability if the method.

(1) I would be interested in a brief discussion on how the HVSR (Horizontal-to-Vertical Spectral Ratio) method is related to the modal analysis of single component seismic data. In case of HVSR, the argument often used is that normalizing the horizontal spectrum by the vertical will reduce the source effects and thus enhance the resonance spectrum of the site. HVSR peaks are interpreted either as SH wave resonance (see equation on Page 6, line 190) or maxima of the Rayleigh wave ellipticity in a layered medium. Would it make sense to present the results of this study as HVSR time-lapse spectra instead of single component spectra (assuming the three-component seismometer have been used)? I would expect to see the same temporal variability by potentially reducing at the same time some spectral peaks related to local sources. Is the 3D nature of the rock glacier the reason for not using spectral ratios?

➔ We understand well this comment, because the HVSR method is now commonly used. However, we used only one-component seismometers that measure vertical movement (we then measure only Rayleigh waves, but they are supposed to dominate surface waves). We precise in the new version: "*The seismometers (Mark Products L4C, one vertical component)*". Indeed, we didn't specified clarly that our seismometers were single (vertical) component, so that the HSVR method was inapplicable in our case. However, we added some mentions to previous publications on this method performed on permafrost, since the methodology is very similar to ours.

(2) The ability of the HVSR method for time-lapse permafrost monitoring has been recently investigated in a few studies:

Abbott, R., Knox, H. A., James, S., Lee, R., and Cole, C.: Permafrost Active Layer Seismic Interferometry Experiment (PALSIE), Tech. rep., Sandia National Laboratories (SNL-NM), Albuquerque, NM (United States), available at: https://prod.sandia.gov/techlib/access-control.cgi/2016/160167.pdf (last access: 7 January 2019), 2016.

Kula, D., Olszewska, D., Dobiński, W., and Glazer, M.: Horizontal-to-vertical spectral ratio variability in the presence of permafrost, Geophys. J. Int., 214, 219–231, https://doi.org/10.1093/gji/ggy118, 2018.

Köhler, A. and Weidle, C.: Potentials and pitfalls of permafrost active layer monitoring using the HVSR method: a case study in Svalbard, Earth Surf. Dynam., 7, 1–16, https://doi.org/10.5194/esurf-7-1-2019 , 2019.

It might be useful to have a look at these studies. Please feel free to not cite them if they are not relevant for the current work (especially since a paper of mine is included).

➔ We were very grateful for sharing these other references, and added some on polar permafrost into our new version. Indeed the HVSR method is broadly used with strong similarities to our spectral analysis, making the parallel relevant. We added this sentence : "*Furthermore, time-lapse monitoring using Horizontal-to-Vertical Spectral Ratio (HSVR) method has already been applied to polar permafrost areas, showing a detectable influence of seasonal variability in the active layer on spectral content of recordings (Köhler and Weidle, 2019; Kula et al., 2018)*."

(3) I miss a figure directly comparing the temporal evolution of the measured resonance frequencies with the modeled once for different states of thawing. Furthermore, a figure comparing the measured and modeled amplitudes spectrum for a particular time would be very useful (for example overlaying figure 2d). In my opinion such figures are more important for demonstrating the reliability of the method than showing the GPR and active seismic results in Fig 4,5 and 6. Those can be moved to the Appendix.

➔ We agree with this comment. This temporal modelling may clearly strengthen the interpretation of our results and improve our publication, but actually we cannot address correctly the transition between seasons. In fact we focus more on the general difference between summer (assuming a complete thawing of the active layer marked by lower values of resonance frequency), and winter (complete freezing of the medium between the surface and the ZAA depth, marked by higher values of resonance frequency). We show the comparison between these extreme values on Figure 13 (winter and summer), but no modelling of the temporal evolution between seasons is proposed. Indeed, a complex thermo-mechanical coupling is required in order to simulate the propagation of the heat wave, but diffusivity properties are poorly known (lack of thermal data from boreholes). In addition, the advection of heat from water adds complexity, and too many assumptions are then required in order to correctly model the time series of resonance frequency using a poroelastic model. Therefore we wouldn't propose this modelling in this publication, even though it should be suggested for future works. The goal of Figure 14 is simply to interpret the relation between ground surface temperature and measured frequencies over the whole year, without any modelling.
The modeled amplitudes spectrum for a particular time would be difficult to compare with the measured one, since 2D and 3D effects on frequency spectrum may appear (see Preiswerk et al. (2019) *(doi: 10.1017/aog.2018.27*). These effects may be very difficult to assess and to predict for rock glaciers (not studied for now). In this article, we focus on the resonance frequency of the fundamental vibrating mode of the rock glacier (at around 15-20 Hz), rather than on the whole amplitude spectrum. But we specified in the first manuscript the complete methodology of the mechanical modelling performed thanks to Comsol software (shown in Figure 12): the computed Frequency Response Function (FRF) is able to model the fundamental mode of the whole structure, but local 2D and 3D effects may affect this curve, making difficult the comparison between modeled and measured curves.

➔ Concerning the GPR and active seismic figures, they should be moved to the appendix session if the editor will consider that there is too many figures in the main part. Indeed this article focus on passive seismic methods and modal analysis, rather than general geophysics results on rock glaciers.

Minor comments:

General: Please check if all commas are needed.

The first sentence of the abstract and the Introduction are identical. Please consider rephrasing.

➔ We changed the first sentence of the introduction, as follows: "*Among periglacial landforms, rock glaciers are tongue-shaped permafrost bodies*."

Line 42: highly challenging?

➔ Yes, replaced.

Line 49: Do you mean "coast-intensive"? Or "…remain cost-effective only when limited to one single …"?

➔ We specified "*cost-intensive and limited to one single point*", as we mean.

Line 61: active permafrost layer

➔ By "surface layers", we want to refer to the active layer, but also the deeper one (until around 10 m depth), which is called permafrost layer since it is composed of permanently frozen materials.

Line 73: Please explain "as a bending beam"

➔ We specified : "*as buildings*", in order to suggest a vertical structure fixed at the bottom.

Line 76: "Our goal … of the rock glacier and the time variability of their resonance frequencies which gives hints …"

➔ Ok.

Line 78-79: "… are numerically modeled …"

➔ Ok.

Line 81: "In the second part, …"

➔ Ok.

Line 97: Something is wrong with formatting of exponents

➔ Ok.

Line 123: one bracket too much

➔ Ok.

Line 130: Are these three-component sensors? Was maintenance required during the measurements (releveling etc.)?

➔ We specify in the new version: "*The seismometers (Mark Products L4C, one vertical component)*". For the maintenance required, we already mentioned that the sensors are subject to tilting, forcing to frequent site visits in order to releveling them.

Line 140: I think the time-lapse resonance spectra of the other sensors should be included as supporting materials or in the appendix (do not need to be discussed)

➔ We agree. However, since the numbers of figures and appendixes are already high, we share the figures of spectrograms from other sensors (Laurichard sensors C01, C03 and

C04) only in personal communication for the moment (see the figures joined). For us it is not necessary to add them into the article, since these data are not interpretable due to tilting and technical instrumentation issues (specified in the text of the manuscript). Please let us know if you want to include them in an additional appendix.

Line 167: “Continuous seismic monitoring systems are composed …” (?)

➔ We change the verb: "*Continuous seismic monitoring requires autonomous operating systems composed of...*".

Line 171: “… between several sensors and to monitor …”

➔ Ok.

Line 195: I suppose the vertical component is used?

➔ Yes, we used seismometers with only the vertical component. We precise it: "*We pre-processed hourly raw seismic traces from vertical component of seismometers*".

Line 200: This is unclear. Please rephrase to describe how peaks are picked automatically.

➔ Ok, we specified exact values of threshold and tried to explain better the picking : “*We selected automatically significant and sharp peaks of the spectrum by using different threshold values for local maxima picking (minimum of peak frequency at 10Hz, minimum of inter-peak distance at 4 Hz, maximum of width of 8 Hz, minimum of peak height at 0.2 and minimum of prominence at 0.3 for normalized spectra).”*

Line 261: Just to avoid misunderstanding: Is the modelling of resonance frequencies done in full 3D, 2D or for a particular location and 1D model below?

➔ In this article we handle the modelling of rock glacier in 1D for particular location underneath seismic sensors. The 2D and 3D effects are quite difficult to address (see Preiswerk, L.E., Michel, C., Walter, F., Fäh, D., 2019. Effects of geometry on the seismic wavefield of Alpine glaciers. Annals of Glaciology 60, 112–124. https://doi.org/10.1017/aog.2018.27). But we checked that resonance frequency of fundamental mode of the 2D model is similar to the one of our simplified 1D models. We detailed this methodology further (part 4.4).

Line 267: “cost-effective” See above.

➔ We replaced by "*cost-intensive*".

Lines 376, 409, 449, and 452: paragraph/section numbers wrong

➔ Ok.

Line 476: “inter-annual climate variability” Is “climate” the right word here? I guess the constant climate at a particular site includes the inter-annual variability of temperatures.

➔ Yes, we agree with this statement. We then modified the first sentences of this paragraph in order to precise what we handle : "*By tracking resonance frequencies in long term, we are able to detect an inter-annual variability. Interestingly, the freezing process appears to correlate with annual minimum of resonance frequency: as an example,* (...)"

Line 491: “observed gap” Do you mean “observed difference”?

➔ Yes, replaced.

Line 496: “in combination with”?

➔ Ok.

Line 498: Remove “Furthermore”

➔ Ok.

Line 515: Sentence “Frequency resonance focuses on …”: I am not sure if this is correctly formulated. The resonance frequency in general is also an effect of seismic waves propagating through the whole structure. It just depends on the considered frequency band. Here, I agree with your conclusion that resonance works well at high frequencies (and thus for shallower depths) where most of the changes occur, while noise correlation does not work so well due to lack of correlation at high frequencies if the inter-station distance is too large. So, the different sensitivities are mainly because of the nature of the ambient noise wavefield and the sensor network set-up, not because of the depth sensitivity of both methods as such. See for example the study of James et al, where noise correlation could be used to measure very shallow variability with closely located sensors.

➔ We specified these statements into the paragraph : "*Furthermore, ambient noise correlation may provide less stable results at high frequencies (up to 14 Hz, for the Gugla study (Guillemot et al., 2020)), preventing any interpretation of the chaotic results due to the lack of high frequency noise in the cross-correlation large inter-sensor distance. Hence, the sensitivity of the different methods depends also on the nature of the ambient noise wavefield together with the sensor network setup. According to the site and its instrumentation, the two passive seismic methods may be combined to obtain stable results along the whole depth of the rock glacier.* "

Line 542: geophysical measurements

➔ Ok.

Appendix A: I am not sure if it necessary to include the results of earthquakes since the results are not much discussed. If they are included, one would like to know where the discrepancy compared to noise comes from.

➔ We decided to keep this figure in Appendix B, because these results are also used as an argument for another discussion. Indeed, we added a new paragraph (in part. 3.2) to handle the question raised about the noise source variability, and its influence on frequency temporal variability.

Figure 2: Showing the noise waveform record is not necessary in my opinion. Instead, please also add a plot like (d) for Gugla.

➔ On our opinion, the Figure 2 eases to show the methodology of frequency picking from a spectrogram of an earthquake. This shows only an example of waveform from an earthquake occurred near the Laurichard rock glacier. The principle for Gugla is strictly the same, therefore a plot for Gugla may overload the figure. In addition, the substantial number of figures and appendixes in this article may be limited, but let us know if you still require this added plot.

Reply to reviews on the manuscript
Modal sensitivity of rock glaciers to elastic changes from spectral seismic noise monitoring and modeling

By Antoine Guillemot, Laurent Baillet, Stéphane Garambois, Xavier Bodin, Agnès Helmstetter, Raphaël Mayoraz, Eric Larose

Contact :
Antoine GUILLEMOT
ISTerre, Université Grenoble Alpes
Grenoble (France)
antoine.guillemot@univ-grenoble-alpes.fr

Dear reviewer, dear editor,

We would like to thank you for the constructive review following the submission of our manuscript "***Modal sensitivity of rock glaciers to elastic changes from spectral seismic noise monitoring and modeling***" to *The Cryosphere*. We took into account all the comments from the two reviewers and editor.

One of the main problems raised concerns the influence of ambient noise sources on resonance frequencies that we picked. Indeed, temporal variability of these frequencies could be related with source variability. To address and discuss this relevant question, we kept the figure showing the spectrograms with frequency picking from earthquakes, in order to show that resonance frequency that we picked are still often visible even for variable earthquake sources. Besides, we added a new figure of spectrograms from a station near the Laurichard rock glacier, settled on a stable site that could be considered as a reference station.

Furthermore, you suggested additional figures to demonstrate the feasability of our method, showing the temporal evolution of modeled resonance frequencies? Unfortunately, this is out of the scope of this publication to our mind, because of the lack of information concerning thermo-mechanical coupling to accurately address this question. We detailed this point further in our response. Nevertheless, we added a new figure in appendix showing the ground surface temperature data, as you requested.

As suggested by the reviewers, we also modified some sentences and figures in order to improve both the quality of information that we provide and the readability of the publication. We added also some references to publications about seismic monitoring on permafrost and glaciers, as a completed state of art.

Please find below a point-by-point response to all your comments (our answers in red), in complement to the new manuscript with highlighted main changes (text in red as well).

Sincerely yours,

On behalf of the authors,

Antoine Guillemot

Comments reviewer 2

The study presents a new methodology that uses the resonant frequency of rock glaciers extracted from continuous ambient noise records to monitor the seasonal and interannual changes in the structure of the vibrating glacier. The seismic modal analysis is coupled to a poroelastic model of a 2D porous medium representing the rock glacier, supported by other geophysical measurements. The results indicate the thawing-freezing cycle effects on the resonance of the glacier. This comprehensive study highlights well how the structural changes of rock glaciers can be tracked and monitored with passive seismology, when other geophysical methods are time-consuming and hardly repeatable at such time resolution.

Major comments:

(1) I miss somewhere an explanation of the origin of the ambient seismic noise (at frequency > 1Hz). Many studies agree to say that it takes its origin in fluvial processes when the water flow from ice melting in spring/summer creates transient forces on the Earth at the glacier base or on the surrounding ice in englacial channels. The noise recorded in winter may come from other sources in the area. Many studies on ambient noise suggest that a change in the noise sources could lead to a change in the noise spectrum. This renders monitoring studies difficult, especially for ambient noise correlation method. Here you use a modal analysis which should be less sensitive to noise source changes. But still, there remains an open question: are the seasonal variations of the resonant frequencies influenced by changes in the noise or actual structural changes ? I am quite concerned about the abrupt resonant frequency shift you observe at the onset of the melting. Personally, I am absolutely confident in the interpretation of actual changes in elastic properties of the structure underneath the sensor. However, this question should be raised and discussed.

- ➔ Thanks for this comment, we addressed and discussed this relevant question in the new version. We already studied the noise source variability, because actually melting processes occurring in spring/summer time can affect the nature of ambient noise, and could lead to spurious comparison of spectral content.
- ➔ During all the year, ambient noise is assumed to be mainly produced by weathering (rain, wind) and anthropogenic sources (traffic on the road in Lautaret Pass for Laurichard, and traffic and human activities in Mattertal valley just below the Gugla rock glacier). In melting and summer periods, noise level is generally higher than during winter time, due to the addition of fluvial and groundwater processes in vicinity of our sites.
- ➔ We addressed this question by adding a new paragraph, and a figure (Fig. 19) in a new Appendix (C). We compared raw and normalized spectrograms of seismic recordings on rock glaciers and on a stable site located in the vicinity. We then presented the results for the OGSA station, located at Lautaret pass (2 km from Laurichard rock glacier) in 2019 (see Fig. 19). From these raw spectrograms we observed a seasonal variability of noise level, actually suggesting a seasonal variability of the noise sources (higher in summer than in winter, probably due to intensified road traffic and fluvial processes in summer). From the normalized spectrograms, we noticed that no significant changes of frequency peaks appear within the illuminated spectrum of interest (10-40 Hz). Since the OGSA station (stable reference) is located close to the Laurichard rock glacier, we assume that ambient noise sources are the same for both sites. Therefore we conclude

that seasonal variability of frequency peaks recorded on the rock glacier between 15 and 40 Hz (see Figure 3) is not much influenced by source changes, but rather linked to specific resonance of the rock glacier structure.

➔ In addition, we chose to keep Figure 18 in Appendix B, showing spectrograms and frequency picking from several earthquakes signals (hence several sources), in order to show that resonance frequency that we picked are still often visible, even for variable earthquake sources.

➔ We detailed all these observations in the new version: "*The spectral content of seismic recordings can be affected by temporal variations of ambient seismic noise sources. For the two sites, these sources are assumed to originate from stable human activities located in the nearby valley and from weathering, but they could also be partly related to hydrological processes via melting water in spring and summer time. This source variability has to be addressed, in order to eliminate any spurious interpretation of actual changes in elastic properties. We then compare raw and normalized spectrograms of the reference station OGSA over one year (see Fig. 19 in Appendix C) to track any variation of the spectrum content which would prevent further comparison of frequency peaks observed on the rock glacier over time. No significant temporal changes of PSD appears within the illuminated spectrum of this stable station located near Laurichard rock glacier. Another obvious fact to highlight is that frequencies which were picked from ambient noise are also often visible when earthquakes signals are considered (see Appendix B). These two observations strengthen the direct link between these frequency peaks and rock glacier resonance".*

➔ In this way we hope that this question of ambient noise sources variability is now correctly addressed and discussed.

(2) As a proof of concept and to approve the interpretation of the results, I suggest to try to actually reproduce the seasonal variations of the resonant frequencies with the poroelastic model (as stated in the conclusion Line 542 but wrong). This would strengthen the discussion and the capability of the method. The interpretation is finally based on Fig 14 which represents measured resonant frequencies as a function of the temperature of the ground surface, while this temperature does not tell the whole story on what is happening at depth. So having a hint on the evolution of the active layer and the rigidity of the structure thanks to the best-fitting model output would definitely strengthen your conclusions. In addition, this figure would be very great to track the interannual changes. Finally, I miss a figure showing the temperature time-series (in this additional « proof of concept » figure, or in Fig 3 for example). This would ease the reading of Fig 14 and also highlight melting seasons versus winter.

➔ Yes, we agree with this comment. This temporal modelling may clearly strengthen the interpretation of our results and improve our publication, but actually we cannot address correctly the transition between seasons. In fact we focus more on the general difference between summer (assuming a complete thawing of the active layer, marked by lower values of resonance frequency), and winter (complete freezing of the medium between the surface and the ZAA depth, marked by higher values of resonance frequency). We show the comparison between these extreme values on Figure 13. (winter and summer), but no modelling of the temporal evolution between seasons is proposed. Indeed, a complex thermo-mechanical coupling is needed in order to simulate the propagation of the heat wave, but diffusivity properties of rock glaciers are poorly known (lack of thermal data from boreholes). In addition, the advection of heat from water adds complexity, and too many assumptions are then required in order to model the time series of resonance frequency by the poroelastic model. Therefore we wouldn't propose

this modelling in this publication, even though it should be suggested for future works. The goal of Figure 14 is simply to interpret the relation between ground surface temperature and measured frequencies over the whole year, without any modelling. Nevertheless, we decided to add a new appendix with a figure showing the temperature time-series in Laurichard, as you requested.

(3) Sometimes, I think that the structure of the sentences is not smooth enough and lead to confusing statements in English. I have listed some in the comments below which need to be reformulate. In general you should try to keep the sentences short.

➔ Yes, we tried to reformulate and shorten the sentences as possible, together with the corrections of some statements you raised below.

Other comments:

L48: in depth -> at depth ?

➔ Ok.

L57-59: References are needed here for both methods (ambient noise vs microseismicity). I understand this is the output of the study by Guillemot et al 2020 as detailed in the following sentence, but other studies have also proven this in glaciated environment.

➔ Yes, we understand the requirement. We completed the references in the new version as follow: "*Passive seismic monitoring systems have the potential to overcome these difficulties on debris slope (Samuel Weber et al., 2018; S. Weber et al., 2018), glaciated (Mordret et al., 2016; Preiswerk and Walter, 2018) and permafrost environments (James et al., 2019; Köhler and Weidle, 2019; Kula et al., 2018), also recently illustrated on the Gugla rock glacier (Guillemot et al., 2020).*"

L89: I suggest to specify « France » after the « Laurichard catchment » Figure 1d: Please indicate the flow direction with an arrow.

➔ Ok.

Section 2.1.3: How were the seismometers maintained (leveling, orientation) ? Are they threecomponent sensors ?

➔ We only used one-component seismometers that measure vertical movement (Rayleigh waves are supposed to dominate surface waves). We precise in the new version: "*The seismometers (Mark Products L4C, one vertical component)".*

You should also specify somewhere here the glacier thickness beneath the stations (ice thickness was also not specified in the previous section)

➔ We guess you addressed the bedrock depth rather than the ice thickness, since rock glaciers are rocky debris bodies. For each sensor and sites (Gugla and Laurichard) we estimated the bedrock depth from different methods (borehole data for Gugla, geophysics for Laurichard) much detailed in the following parts.

L137: « The long periods » -> the longest periods ?

➔ Ok.

L139: What is the distance between these two stations ?

➔ We precise in the text : "*Therefore we decided here to present results from only these two locations, separated by around 80 m*".

L140: It could be interesting to have the results for the seismic measurements at the other stations in the appendix.

➔ Yes, we agree. But since the numbers of figures and appendixes are already high, we share the figures of spectrograms from other sensors (Laurichard sensors C01, C03 and C04) only in personal communication for the moment (see the figures joined). For us it is not necessary to add them into the article, since these data are not interpretable due to tilting and technical instrumentation issues (specified in the text of the manuscript). Please let us know if you want to include them in another appendix.

L144: I suggest to specify « Switzerland » after « Wallis Alps »

➔ Ok.

L157: Please specify here if the geophones are one or 3 components. Are they deployed directly on the ice ? Were they maintained ?

➔ We only used one-component seismometers that measure vertical movement (Rayleigh waves are supposed to dominate surface waves). We precise in the new version: "*The seismometers (Mark Products L4C, one vertical component)"*. These sensors are settled on top of relatively large, stable and flat boulders, and sheltered by a plastic tube to shield off any influence of rain, wind and snow. They are connected together with wires insulated by sheath to protect for weather and rockfalls. All these details about instrumentation are in the manuscript.

L169-171: This is the right place to be more specific for glacier microseismicity and glaciological applications (location of crevasses, basal interface and asperities, water channels) with appropriate referencing. For ambient noise studies on glaciers, you could refer to the studies of Preiswerk and Walter 2018, Sergeant et al 2020 (for the imaging part) and Lindner et al 2018 (for the monitoring part)

Preiswerk, L. E., & Walter, F. (2018). High-Frequency (> 2 Hz) Ambient Seismic Noise on High- Melt Glaciers: Green's Function Estimation and Source Characterization. *Journal of Geophysical Research: Earth Surface*, *123*(8), 1667-1681.

Sergeant, Amandine, et al. "On the Green's function emergence from interferometry of seismic wave fields generated in high-melt glaciers: implications for passive imaging and monitoring." *The Cryosphere* 14.3 (2020): 1139-1171.

Lindner, F., Weemstra, C., Walter, F., & Hadziioannou, C. (2018). Towards monitoring the englacial fracture state using virtual-reflector seismology. *Geophysical Journal International*, *214*(2), 825-844.

➔ Thanks a lot for sharing these references. We added several of them in order to complete the former state of art: "*Passive seismic monitoring systems have the potential to overcome these difficulties on debris slope (Samuel Weber et al., 2018; S. Weber et al., 2018), glaciated (Mordret et al., 2016; Preiswerk and Walter, 2018) and permafrost environments (James et al., 2019; Köhler and Weidle, 2019; Kula et al., 2018)*" But since rock glaciers behave rather like rocky landslides than glaciers, we wouldn't favor references on glaciological applications rather than others. We focus more on references

about spectral analysis of ambient noise recordings on glacial and periglacial environments.

L171: add « to » before monitor.

➔ Ok.

L174: « on it » -> « on site »

➔ Ok.

L176: « tracking dynamic parameters » -> « tracking the evolution of »

➔ Ok.

L180: « The seismic noise averaging properties » What does this refer to ?

➔ We modify the sentence to precise what property is in question: "*Through stacking source and trajectories over time and space, seismic noise allows considering the illuminated frequency spectrum as large and stable enough to overcome these respective effects, particularly when monitoring is considered.* "

L182: « The PSD is simply defined by averaging the intensity of the FFT » You average it by what ? The (inverse of) time of integration ? I do not see any averaging in the proposed equation.

➔ We wanted to mention that we stacked the seismic frequency content over time (hourly or daily) before computing the PSD ; that's why we considered a time-averaging. But we already precised that we process hourly raw data in the previous version, so that we remove this mention here : "*The power spectrum density (PSD) is simply defined by computing the intensity of the fast Fourier transform (FFT) of the seismic record*".

L185. Preiswerk et al 2019 also investigated the resonant glaciers with different geometries which imply 1D, 2D and 3D resonances through HVSR, time-frequency dependent polarization and modal analysis. This study should be cited, here maybe or elsewhere.

Preiswerk, L. E., Michel, C., Walter, F., & Fäh, D. (2019). Effects of geometry on the seismic wavefield of Alpine glaciers. *Annals of Glaciology*, *60*(79), 112-124.

➔ Thanks for sharing these relevant reference. We actually mentioned it twice in the new version (in methods of spectral analysis of seismic data (part. 3.1) "*The estimation of bed geometry properties from spectral analysis of seismic noise has already been studied on alpine glaciers (Preiswerk et al., 2019)*", and modal analysis and frequency response of the rock glacier (part 4.4) "*Similar to the fundamental mode of an unstable rock mass (Burjánek et al., 2012) and avalanche glaciers (Preiswerk et al., 2019), the measured polarization is almost linear*".

L191: « in absence of geometrical changes » maybe specify here « (i.e. ablation/accumulation) »

➔ Yes, we agree. In a case of rock glacier, the potential geometrical changes may be related rather to an intensive creeping movement (or a destabilization), than to accumulation or ablation (like glaciers). Then we precise this with accurate words for rock glaciers: "*Extending this approach to a rock glacier shows that in absence of*

geometrical changes (no significant destabilization), resonance frequency variations can be related to evolution of its rigidity, through Young's modulus and density".

L191: missing comma after Young's modulus.

➔ Ok.

L195: Which component ?

➔ We precise in the new version: "we pre-processed hourly raw seismic traces from vertical-component seismometers".

L200-204: The picking method is not clearly described. Additionally, please specify why you expect to have frequency peaks above 10 Hz on the glacier ? Is it related to the glacier morphology and more specifically to the ice thickness ?

➔ We rewrite this part to clarify some points. We precise the values of threshold : "*We selected automatically significant and sharp peaks of the spectrum by using different threshold values for local maxima picking (minimum of peak frequency at 10Hz, minimum of inter-peak distance at 4 Hz, maximum of width of 8 Hz, minimum of peak height at 0.2 and minimum of prominence at 0.3 for normalized spectra)*."

➔ We don't expect to see any resonance frequency of the rock glacier below 10 Hz, after viewing the spectrograms of all sensors on the two sites. Furthermore, for a simplified 1D model with soft rock glacier on hard bedrock, the frequency of the fundamental mode would be f0=Vs/4h (mentioned in the article). With h= 10m and Vs=600m/s (orders of magnitude), peaks below 10 Hz would be unlikely for specific resonance of the whole rock glacier body.

Figure 2d: It seems that you still see the 23 Hz anthropogenic peak at station C05 (as expected) but it is not obvious because of the normalization. Maybe indicate this in the caption.

➔ Yes, we indicated this in the caption.

L212: « The results of PSD » -> « The spectrograms of PSDs »

➔ Ok.

L218: « no subglacial resonating water-filled cavities was known on the site ». I suspect you refer to moulins which extend from the glacier surface to (probably) the glacier base (this is what it sounds as you cite Röösli et al 2016) ? If yes, the part of the sentence Line 2018 should me modified to point out to moulins. If no, how do you know that there is absolutely no channels in the glacier ?

➔ Yes, we agree with that. We then modified the sentences to clarify the two hypotheses (hydrological because groundwater can exist, even if depth and location are unknown, and anthropological) : "*Since this frequency peak is fully stable over time, we interpret its origin as either hydrological or anthropogenic. It may be generated either by groundwater flow within the rock glacier (Roeoesli et al., 2016), or by a pressure pipe located 400 m downstream or from road traffic coupled with a tunnel near the Lautaret pass (see Fig. 1). This frequency peak is also visible on spectrograms of station OGSA (see black arrow in Fig. 2d) located at Col du Lautaret on a stable site, suggesting a potential anthropogenic source. The spectral content of these recordings exhibits the same peak at 23-24 Hz (see red curve in Fig. 2d), implying it is not directly related to*

the rock glacier resonance. Then this frequency peak is hereafter excluded from the analysis".

L225: « resonating structure of the sensor » -> « beneath the sensor » ? Do you refer to the glacier or the shelter around the sensor ?

➔ We referred to the shelter around and above the sensor (precise in the new version).

Section 3.2: see major comment: I miss somewhere an explanation of the origin of the ambient seismic noise (at frequency > 1Hz). Many studies agree to say that it takes its origin in fluvial processes when the water flow from ice melting in spring/summer creates transient forces on the Earth at the glacier base or on the surrounding ice in englacial channels. You say later (Line 224) that water filling of the resonating structure could be responsible for changes in PSD. Then you say Line 229 that no water was present in the sensor settlement. In fact, the presence of meltwater inside the glacier does affect the seismic noise with strong noise generated in spring/summer and little englacial noise in winter. The noise recorded in winter may come from other sources in the area. This should appear on non-normalized spectrograms. In this case, there remains an open question on the cause of the resonating frequency shift from winter to summer. Is it related to source effects or structural changes ? I am confident in the interpretation of actual changes in elastic properties of the structure underneath the sensor. However, this question should be raised at the end of this section or in the discussion.

➔ Yes, we address this question (see major comment above). The new paragraph that we added is : "*The spectral content of seismic recordings can be affected by temporal variations of ambient seismic noise sources. For the two sites, these sources are assumed to originate from stable human activities located in the nearby valley and from weathering, but they could also be partly related to hydrological processes via melting water in spring and summer time. This source variability has to be addressed, in order to eliminate any spurious interpretation of actual changes in elastic properties. We then compare raw and normalized spectrograms of the reference station OGSA over one year (see Fig. 19 in Appendix C) to track any variation of the spectrum content which would prevent further comparison of frequency peaks observed on the rock glacier over time. No significant temporal changes of PSD appears within the illuminated spectrum of this stable station located near Laurichard rock glacier. Another obvious fact to highlight is that frequencies which were picked from ambient noise are also often visible when earthquakes signals are considered (see Appendix B). These two observations strengthen the direct link between these frequency peaks and rock glacier resonance*."

➔ ". We also added a new Appendix (B) with a figure to show and clarify this point.

Figures 3/4: The blue boxes indicating the melting season are present only for spring. On what observations is it based on ? Generally in Alpine glaciers, the melting seasons spread from spring (April/May) to the end of summer (september/october).This would also be consistent with the seasonal cycle you observe for the seismic dominant frequency. Also related to this comment, I would say in Line 233: « a sudden drop of frequency occurs at the time when melting processes [start to occur in spring and stay stable to lower frequency over the course of the summer]. »

➔ Melting periods are defined based on thermal data acquired on thermistors located at the ground (around 10 cm depth) surface around the rock glacier. They are limited to the period when the "zero-curtain effect" (temperature constant and equals to the

freezing point) is visible, which highlights the partial refreezing of melting water. We added a new figure showing these data in Appendix (Figure 16) in order to clarify this point. When the temperature goes up to positive values, we consider that the melting period is finished, since active layer is totally thawed until the surface. But of course, melting water from upstream still remains, extending the "melting period" to the end of summer, in a sense that you suggest.

Figures 3-4: I would here display the time series of air or ground temperature + periods of snow cover. This would ease the interpretation in the discussion and Fig 14

➔ Yes, we decided to add a new appendix with a figure showing the temperature time-series in Laurichard (Figure 16), as you requested.

Figure 4: Nice observation !

Line 247: I would add « at [spring and] summer time »

➔ Ok.

Line 261: Do you have a reference for the software ?

➔ Yes, we added a reference as bottom of page : " COMSOL Multiphysics® v. 5.4, www.comsol.com, ComsolLab, Stockholm, Sweden."

Figures 5-7: I suggest to move these figures to the appendix section as I think that the study should be focused on the modal analys/modeling methodology.

➔ Ok, we agree. These figures should be moved to the appendix session if the editor will consider that there is too many figures in the main part. Indeed this article focus on passive seismic methods and modal analysis, rather than general geophysics results on rock glaciers.

Line 391: « appling » -> applying

➔ Ok.

Line 446: « as shown in Fig 13 for Laurichard and not presented here but similar for Gugla » Results for both glaciers are presented in Fig 13, so you should revise this sentence.

➔ Ok, we removed this sentence.

Line 449: Section number missing (and elsewhere)

➔ Ok, checked.

Line 450: « and compare them to the maximum values of the observed ones ». You should indicate here that data are indicated by squares and rephrase this as the text alone is confusing. Say that you represent here the maximum and minimum bounds of the resonance frequencies you measure for each mode, for the two years - if I understand correctly.

➔ Yes, you understand correctly the Figure 13. But we clarify the text to prevent confusion : "*We compare them to the maximum (in winter) and minimum (in summer) values observed on all sites (depicted in squares in Fig. 13, values from Fig. 3 for Laurichard and Fig. 4 for Gugla).* "

Line 452-453: « Resonance frequencies of these modes match the freq band of measurements below 50 Hz, and generally decrease with thawing ». There is no relation between the two parts of this sentence so you should split it in two. The first part is a bit redundant with the previous sentence of the text. In general I think that section 4.5 could be better rewritten and reorganized with clearer description of the glacier seismic behavior.

➔ Yes, we reorganized a bit this paragraph. This sentence has been moved before, as it deals with general statements about expected resonance frequency.

Line 454: I would add at the end after « for all cases » « i.e. Gugla and Laurichard »

➔ Ok, added.

Line 455: You should remind here that C05 is towards the glacier tongue (on thinner ice H=8m according to your velocity model) and C00 is more upstream (H=14 m).

➔ It is not about ice thickness (unknown here), but rather about bedrock depth. This major difference between sensors C00 and C05 is reminded in this paragraph.

Figure 13: You could add arrows: one which points toward higher depths of thawing indicating summer, one which points toward 0 indicating winter

➔ Ok, we modified Figure 13 as requested.

Line 465: I would replace « melting periods » by « at the onset of the melting period in spring » (summer is also a melting period).

➔ Yes, we replaced this expression by: "*a sudden drop at the onset of melting periods in spring and lower values during summers*".

Line 471: « observed seasonal freq variations » -> observed freq seasonal variations

➔ Ok.

Lines 487-488: « in 2019 … frequency is lower than is 2018 » Give values !!

➔ We precise: "*Similarly for the Gugla site, the winter resonance frequency was significantly lower in 2017 (19 Hz) than in the others years (around 23 Hz).*"

Line 488: « In addition to an earlier snow cover period in 2019 than 2018 … » I would reformulate. Did snow falls started earlier in 2019 or was the period for snow cover shifted earlier in time ? « frozen » -> « refrozen » ?

➔ We reformulated : "*earlier and longer snow cover in 2019 than in 2018*".

Lines 475-489: I think this paragraph could be improved with some reorganization. You should highlight your conclusion which is that, on average, resonance frequencies are more sensitive to the intensity of internal thawing (which is influenced by …) than to the air temperature as … Also you use both the present and the past to describe the observations. You should homogenize this.

➔ We homogenized this paragraph and tried to clarify the examples together with the main message in conclusion.

Could you explain those differences with your model ? Can different level of porosity and depth of thawing mimic different intensity of thawing ? It would be very great to have a figure

showing the time series of the observed resonance frequencies with the model results for different states of thawing.

➔ This request is already discussed as a major comment above. This temporal modelling may clearly strengthen the interpretation of our results and improve our publication, but actually we cannot address correctly the transition between seasons (which state of freezing/thawing correspond to which time ?). We focus more of the extreme values (low values in summer, high values in winter), as depicted in the modified Figure 13.

Lines 489-498: I suggest to remove this paragraph from the discussion which is focused on the thawing-freezing cycle.

➔ We agree that the discussion deals mostly with freezing-thawing cycle, but we wanted to highlight the fruitful benefit of GPR results on the bedrock depth estimation, in combination with passive seismic measurements. Indeed, the difference of bedrock between the two sensors for Laurichard is the unique reason for the gap of resonance frequency amplitude between them. Thus, an accurately estimated bedrock depth is required to finely analyze and model the effect of seasonal thermal forcing on our seismic measurements. Let's us know if you still want to remove this paragraph from the discussion, in this case it can be moved to the appendix section.

Line 499: I would remove « non-linear ».

➔ Ok.

Line 500: « over the year » -> along the year

➔ Ok.

Line 501: I would remove « dry » as we do not know if you are referring to the air or the rock glacier.

➔ Ok.

Lines 521-522: « for ambient noise correlation method, the theoretical relative velocity change of the Rayleigh wave is computed by dispersion curve difference using the Geopsy package» -> I would say « for … corr method, we compute the dispersion curves of the Rayleigh wave using the Geopsy software. The theoretical relative velocity changes are computed by measuring the differences of the dispersion curve with the reference one at each frequency. »

➔ We reformulated: "*for ambient noise correlation method: we compute the dispersion curves of the Rayleigh waves using the Geopsy package (Wathelet et al., 2004). The theoretical relative velocity changes (dV/V) are computed by measuring the difference between the modified dispersion curve with the reference one at each frequency*".

Figure 15: For the modal analysis, you say « first mode » while everywhere in the text you refer to the fundamental mode. This could be confusing. You should specify the resonance frequency, and also in the main text.

➔ Yes, we changed the "first mode" to "mode 0". Mode 0 is already mentioned in Figure 13 and is commonly used for referring the fundamental mode.

Line 538: I would say « continuous seismic noise measurements »

➔ Ok.

Line 539: This is minor but I would say something like « These freq show seasonal variations that are to be related with changes in elastic properties of the structure underneath the recording sensor, due to freeze-thawing effects ».

➔ Ok, we modified by: "*These frequencies show seasonal variations, related with changes in elastic properties of the structure underneath the recording sensor, due to freeze-thawing effects*".

Line 541: « which fit well the recorded frequencies » I would specify here or next sentence on what the resonance freq depend in the poroelastic model. Basically the take-home message I keep from your analysis is that the freq depend on the maximum depth of thawing in a porous medium.

➔ For us this sentence is a general statement for the good agreement between modeled and measured extreme values of resonance frequency. We detailed below this take-home message (see next comment).

Line 542: « we have reproduced the observed seasonal variations » This is a strong statement, you did not reproduced the seasonal cycle exactly but only reproduce the maximum freq in winter due to maximum freezing and minimum freq in summer due to maximum thawing. See my major comment.

➔ Yes, we precise : "*we have reproduced the observed higher values in winter due to maximum freezing, and lowest values in summer due to maximum thawing*".

Line 551: « insight to other deeper processes » -> into other processes at greater depth

➔ Ok, replaced.

Modal sensitivity of rock glaciers to elastic changes from spectral seismic noise monitoring and modeling

Antoine Guillemot[1], Laurent Baillet[1], Stéphane Garambois[1], Xavier Bodin[2], Agnès Helmstetter[1], Raphaël Mayoraz[3], Eric Larose[1]

[1] Univ. Grenoble Alpes, CNRS, Univ. Savoie Mont-Blanc, IRD, IFSTTAR, ISTerre, 38000 Grenoble, France
[2] Univ. Grenoble Alpes, CNRS, Univ. Savoie Mont-Blanc, Laboratoire Environnements, Dynamiques et Territoire de Montagne (EDYTEM, UMR 5204), 73000 Chambéry, France
[3] Canton of Wallis, 1951 Sion, Switzerland

Correspondence to: A. Guillemot (antoine.guillemot@univ-grenoble-alpes.fr)

Abstract. Among mountainous permafrost landforms, rock glaciers are mostly abundant in periglacial areas, as tongue-shaped heterogeneous bodies. Passive seismic monitoring systems have the potential to provide continuous recordings sensitive to hydro-mechanical parameters of the subsurface. Two active rock glaciers located in the Alps (Gugla, Switzerland and Laurichard, France) have then been instrumented with seismic networks. Here, we analyse the spectral content of ambient noise, in order to study the modal sensitivity of rock glaciers, which is directly linked to elastic properties of the system. For both sites, we succeed in tracking and monitoring resonance frequencies of specific vibrating modes of the rock glaciers during several years. These frequencies show a seasonal pattern characterized by higher frequencies at the end of winters, and lower frequencies in hot periods. We interpret these variations as the effect of the seasonal freeze-thawing cycle on elastic properties of the medium. To assess this assumption, we model both rock glaciers in summer, using seismic velocities constrained by active seismic acquisitions, while bedrock depth is constrained by Ground Penetrating Radar surveys. The variations of elastic properties occurring in winter due to freezing were taken into account thanks to a three-phase Biot-Gassmann poroelastic model, where the rock glacier is considered as a mixture of a solid porous matrix and pores filled by water or ice. Assuming rock glaciers as vibrating structures, we numerically compute the modal response of such mechanical models by a finite-element method. The resulting modeled resonance frequencies fit well the measured ones along seasons, reinforcing the validity of our poroelastic approach. This seismic monitoring allows then a better understanding of location, intensity and timing of freeze-thawing cycles affecting rock glaciers.

1 Introduction

Among periglacial landforms, rock glaciers are tongue-shaped permafrost bodies. They are composed of a mixture of boulders, rocks, ice lenses, fine frozen materials and liquid water, in various proportions (Barsch, 1996; Haeberli et al., 2006). Gravitational and climatic processes combined with creeping mechanisms lead these glaciers to become active, exhibiting surface displacements ranging from cm/yr to several m/yr (Haeberli et al., 2010). In the context of permafrost degradation associated to climate warming, destabilization processes coupled to an increase of available materials are increasingly observed

in a large range of alpine regions (Bodin et al., 2016; Delaloye et al., 2012; Marcer et al., 2019b; Scotti et al., 2017), thus increasing the risk of torrential flows (Kummert et al., 2018; Marcer et al., 2019a). Therefore, monitoring of active rock glaciers has become a crucial issue to understand physical processes that determine rock glacier dynamics, through thermal, mechanical and hydrological forcing (Kenner et al., 2019; Kenner and Magnusson, 2017; Wirz et al., 2016) and consequently to better predict extreme events threatening human activities. Indeed, linking internal mechanisms at work to environmental factors remains poorly constrained (Buchli et al., 2018), and lacks quantitative models constructed from high resolution observations. In this view, rock glacier monitoring is a highly challenging field that has developed over the last decades through several methods (Haeberli et al., 2010). Investigating the internal deformation remains very costly and limited in temporal and spatial scales with geophysical methods and/or borehole investigations (Arenson et al., 2016). Kinematics of the topographical surface is more accessible by remote sensing methods (with terrestrial photogrammetry or laser scanning, aerial or spatial imagery), together with *in situ* measurements (differential GPS, total station) (Bodin et al., 2018; Haeberli et al., 2006; Kaufmann et al., 2019; Strozzi et al., 2020). However, the knowledge of the medium geometry and composition along with its internal processes that drive rock glacier dynamics require more investigations at depth (Springman et al., 2013). Boreholes provide useful data (temperature, composition, deformation along depth) but remain cost-intensive and limited to one single point of observation. By measuring physical properties sensitive to hydro-mechanical parameters of the medium, a wide range of geophysical methods provides interesting tools to characterize and monitor rock glaciers at a larger scale (e. g. Duvillard et al., 2018; Kneisel et al., 2008; Maurer and Hauck, 2007). However, the need of high resolution temporal monitoring reduces the choice of geophysical methods.

Passive seismic monitoring systems have the potential to overcome these difficulties on debris slope (Samuel Weber et al., 2018; S. Weber et al., 2018), glaciated (Mordret et al., 2016; Preiswerk and Walter, 2018) and permafrost environments (James et al., 2019; Köhler and Weidle, 2019; Kula et al., 2018), also recently illustrated on the Gugla rock glacier (Guillemot et al., 2020). Indeed, seismological networks provide continuous recordings of both seismic ambient noise and microseismicity. The former allows us to estimate tiny seismic wave velocity changes associated to hydro-mechanical variations through ambient noise correlation method, while the latter monitors and locates in time and space the seismic signals generated by rockfalls or by internal cracking and deformation. With these techniques, the seasonal freeze/thawing cycles have been monitored on the Gugla rock glacier during four years (Guillemot et al., 2020), by quantitatively measuring the increase of rigidity within the surface layers (active and permafrost layers) during wintertime. Seismic velocity drops have also been observed during melting periods, indicating thawing and water infiltration processes occurring within the rock glacier.

The goal of this study is to extend the freeze-thawing cycle observations previously obtained on a single site from seismic noise correlation (Guillemot et al., 2020) to modal monitoring of two rock glaciers, and evaluate similarities and differences between these two methods. Assuming a rock glacier as a vibrating system, the resonance frequencies that naturally dominate and their corresponding modal shapes should provide information about mechanical parameters of this system. Hence these frequencies and modal parameters are directly linked to elastic properties of the system, which evolve according to its rigidity and its density (Roux et al., 2014). Since decades, such modal analysis and monitoring of structures have been performed using

seismic ambient noise, especially for existing buildings (Guéguen et al., 2017; Michel et al., 2010) and rock slope instabilities (Burjánek et al., 2010; Lévy et al., 2010). Both numerical simulations and laboratory experiments have been already performed with ambient seismic noise sources to confirm the potential of such non-invasive monitoring of modal parameters changes of a structure, as buildings (Roux et al., 2014). Furthermore, time-lapse monitoring using Horizontal-to-Vertical Spectral Ratio (HSVR) method has already been applied to polar permafrost areas, showing a detectable influence of seasonal variability in the active layer on spectral content of recordings (Köhler and Weidle, 2019; Kula et al., 2018). Here, we propose to evaluate the potential of this methodology on two rock glaciers located in the Alps (Laurichard in France and Gugla in Switzerland), at elevations where climatic forcing dominate the variations of their internal structures and consequently their dynamics. We focus on the spectral content of continuous seismic data (noise and earthquakes) to track and monitor resonance frequencies. Our goal is to detect vibrating modes of the rock glacier and the time variability of their resonance frequencies, which gives hints to better quantify and locate the changes of rigidity resulting from freeze-thawing effects on surface layers. These observations are numerically modeled using a finite-element method, towards a mechanical modeling of such rock glaciers.

After presenting the two studied rock glaciers and their instrumentation, we present the methodology to perform a spectral analysis from seismic data, and the resulting resonance frequencies variations observed on both sites. In the second part, we detail the mechanical modeling of those rock glaciers, based on finite-element method and constrained by several geophysical investigations, which allows to compute synthetic resonance frequencies and to understand their sensitivity. Finally, we compare observed and modeled modal studies, in order to converge to a consistent view of those rock glaciers and their freeze-thawing cycles.

2 Presentation of the sites

2.1 The Laurichard rock glacier

2.1.1 Context

As presented in previous studies (Bodin et al., 2018, 2009; Francou and Reynaud, 1992), the Laurichard catchment in France was chosen as a test site for different geomorphological studies conducted since several decades. This large thalweg is part of the Combeynot massif, which is a crystalline subsection of the Ecrins massif located in the South of Lautaret pass. This area constitutes a climatic transition between northern and southern French Alps. Several rock glaciers are observed in this area in different states of deformation, from relicted to active ones. Among them, the Laurichard rock glacier is the most studied active rock glacier in the French Alps ((Bodin et al., 2018; Francou and Reynaud, 1992), Fig. 1a). It appears as a 800 m long and 100-200 m wide tongue-shaped landform of large boulders, flowing downstream between the rooting zone (2650 m a.s.l) and the front zone (2450 m a.s.l). It is fed by the gravitational rock activity that originates on the surrounding slopes, composed of highly fractured granitic rockwalls providing large boulders (10^{-2} – 10^{1} m diameter). It shows rather simple and evident features of active rock glacier morphology (Bodin et al., 2018): transversal ridges and furrows, steeper lateral talus and rock activity at

the front, unstable rock mass on the surface. These geomorphological hints typically reveal creeping movement of the whole debris mass, with the presence of ice mainly responsible for this rock glacier dynamics.

The kinematic behavior of the Laurichard rock glacier has been studied since several decades: large blocks have regularly been marked since 1984 (Francou and Reynaud, 1992) together with other remote sensing techniques or geodetic measurements (total station, Lidar and GPS). The long term survey permits to measure surface velocity with different temporal and spatial scales, reaching very high resolution (below one day and one meter, (Marsy et al., 2018)). The general spatial velocity pattern shows a main central flow line along the maximal slope. At the frontal zone, it appears that the right orographic side is the most active part of the rock glacier. The mean annual surface velocity of the site is measured at around 1m/yr, with a progressive increase between 2005 and 2015, probably in reaction to the observed increase in mean annual air temperature during this period (Bodin et al., 2018). This latter acceleration has been observed synchronously on other monitored rock glaciers in the Alps (Delaloye et al., 2008; Kellerer-Pirklbauer et al., 2018) and is most probably resulting from the warming of the permafrost (Kääb et al., 2007).

2.1.2 Available data and knowledge

The thermal regime of the rock glacier is monitored since 2003 thanks to Miniature Temperature Dataloggers (MTD) that record every hour the temperature of the sub-surface (below 2-10 cm of debris) at five different locations (one being located outside the rock glacier, see Fig. 1a). These time series of ground surface temperature highlight alternating snow cover and melting periods over the whole data period (see Appendix A). Geophysical investigations have been performed several times since 2004, especially with ERT surveys providing a first estimation of the internal structure (ice content and thickness) subject to permafrost degradation (Bodin et al., 2009).

The topography of the rock glacier has also been regularly surveyed since two decades using high-resolution Digital Elevation Models (DEM) computed from terrestrial and remote-sensing methods (Bodin et al., 2018). In this study, a DEM at a 10 m resolution derived from the IGN (French national institute for geographic information) BD Alti product was used. Additionally, a DEM of the bed over which the rock glacier is flowing was interpolated from manually drawn contour lines based on surface DEM. These contour lines of the bed extend the contour lines of the terrain surrounding the rock glacier below its surface, using local constraints from existing geophysical data (Bodin et al., 2009). For this operation, we assume that the rather simple overall morphology of the Laurichard rock glacier (a single relatively narrow tongue) and its overimposed position above surrounding terrain (bedrock and other debris slopes, called “bedrock” below) allow to estimate the lateral thickness variability of the rock glacier. This DEM of the bedrock is coherent with bedrock depth derived from GPR acquisitions conducted in 2019, and thus will be used to constrain Laurichard rock glacier geometry (see section 4.2.1).

2.1.3 Passive seismic monitoring

Since December 2017, an array of six seismometers (named C00 to C05) has been set up on the lower part of the Laurichard rock glacier (Figure 1e). They are located around 50 m apart, covering the whole area of the rock glacier front. The seismometers (Mark Products L4C, one vertical component) are coupled with the top of relatively large, stable and flat boulders, and sheltered by a plastic tube to shield off any influence of rain, wind and snow. They are connected together to one digitizer (Nanometrics Centaur, sampling rate 200 Hz) with wires insulated by sheath to protect from weather and rockfalls. This passive seismological network records continuously ambient noise together with microseismicity.

Because of a rough field context (climatic conditions and surface instability, subjecting sensors to tilting), and although frequently required site visits in order to releveling sensors, the longest periods of usable data have been recorded from only two seismometers: C00 (located around 100 m upstream the front, on the right side of the rock glacier) and C05 (located near the front, on the left side). Therefore we decided here to present results from only these two locations, separated by around 80 m. In the following part, we used these passive seismic recordings to model the dynamic response of the site, through their spectral analysis. Other sensors, though discontinuously active, and not presented here, yield the same observations and conclusions when in operation.

2.2 The Gugla rock glacier

Located in Wallis Alps (Switzerland), the Gugla rock glacier (also called Gugla-Breithorn or Gugla-Bielzug) is part of a large number of active rock glaciers that have been regularly investigated over the last decade in this geographic area (Delaloye *et al.* 2012, Merz *et al.* 2016, Wirz *et al.* 2016, Buchli *et al.* 2018). Ranging from 2550 to 2800 m *asl*, its tongue-shaped morphology covers about 130 m in width, 600 m in length, and is up to 40 m thick in its downstream part. Since 2010, surface velocities have been measured about 5 m/yr at the front, with a peak in the southern part culminating, in 2013, at a velocity of more than 15 m/yr. This increase in velocity has also propagated to the rooting zone (from 0.6 m/yr in 2008 to 2 m/yr in 2018, as evidenced by geodetic measurements). Debris detachments from the rock glacier front supply yearly one or more torrential flows triggered from an area located immediately downslope of the rock glacier front, regularly reaching the main valley downstream with dense human facilities. Hence, the risk of runout onto the village of Herbriggen and railways and roads nearby remains high after intense snowmelt or following long-lasting or repeated rainfall, involving volumes from 500 to more than 5000 m^3 per event (Kummert and Delaloye, 2018).

In addition to meteorological stations and GPS monitoring systems, a seismological network has been set up since October 2015, covering the lower part of the rock glacier (Guillemot et al., 2020). It is composed of five seismic sensors (labelled C1 to C5, Sercel L22 geophones with a resonance frequency of 2 Hz), including two of them (C2 and C4) located on the glacier's longitudinal axis, whereas the others are placed on the two stable sides (Figure 1e).

In addition, eight boreholes and one geophysical campaign from seismic refraction were performed on the rock glacier in 2014 (Geo2X, 2014, CREALP, 2016, 2015) in order to better constrain the internal structure of the subsurface (thickness and composition of the layers, seismic velocity). Through two thermistor chains that have continuously recorded temperature at depth (until 19.5 m) between 2014 and 2017, the active layer thickness has been located at around 4.5 m (+/-20%) (CREALP, 2016). Finally, three webcams provide hourly images showing different viewpoints of the rock glacier front (Kummert et al., 2018).

3 Spectral analysis of seismic data

3.1 Methods

Continuous seismic monitoring requires autonomous operating systems composed of an array of seismometers that permanently record particle vibrations on the ground related to microseismicity and noise. Microseismicity is increasingly used for precisely locating the seismic signals induced by mass movements, avalanches and rockfalls (Spillmann et al., 2007, Amitrano et al., 2010; Helmstetter and Garambois, 2010; Lacroix and Helmstetter, 2011). Ambient seismic noise is widely used to investigate the medium between several sensors and to monitor subsurface properties variations (Snieder and Larose, 2013, Larose et al, 2015, for a review).

Experimental results combined with numerical modeling showed that resonance frequencies of a structure can be derived from the spectral analysis of ambient seismic noise recorded on site (Lévy et al., 2010; Michel et al., 2010). Different applications were successfully proposed: as a monitoring method for a prone-to-fall rock column (Lévy et al., 2010) or as a way of tracking the evolution of dynamic parameters of existing structures. Indeed, ambient vibrations provide information about the modal parameters of a structure, defined as resonance frequencies, modal shapes and damping ratios (Michel et al., 2008). These features can be deduced from the frequency content of seismic recordings, which depends on source and propagation properties, but also on structural, geometrical and elastic properties of the structure (Roux et al., 2014). Through stacking source and trajectories over time and space, seismic noise allows considering the illuminated frequency spectrum as large and stable enough to overcome these respective effects, particularly when monitoring is considered. The power spectrum density (PSD) is simply defined by computing the intensity of the fast Fourier transform (FFT) of the seismic record $\varphi_a(t)$: $PSD(\omega) = |FFT(\varphi_a(t))|^2$, where ω is the angular frequency. In resonant structures like sedimentary basins, rock columns, mountain slopes and buildings, high peaks in the PSD could correspond to specific vibration modal shapes of the structure (Larose et al., 2015). The corresponding frequencies, identified as resonance ones, mainly depend on geometrical (characteristic length, cross-section, shape), structural (boundary conditions) and mechanical (density, Young's modulus) features defining the structure.

As an example, one can approximate a (soft) sedimentary cover overlying a (hard) bedrock using a 2-D semi-infinite half-space covered by a soft layer of density ρ, thickness h, average shear-wave velocity V_s and shear modulus μ. Such simple mechanical modeling leads to the well-known analytic solution of the first resonance frequency f_0 corresponding to the

fundamental mode (Parolai, 2002): $f_0 = \frac{V_S}{4h} = \sqrt{\mu/\rho}/4h$. The estimation of bed geometry properties from spectral analysis of seismic noise has already been studied on alpine glaciers (Preiswerk et al., 2019). Extending this approach to a more heterogeneous rock glacier shows that in the absence of geometrical changes (no significant destabilization), resonance frequency variations can be related to evolution of its rigidity, through Young's modulus, and of its density. In this study, our goal is to track the temporal evolution of resonance frequencies of a rock glacier, considering it as a vibrating structure, in order to understand their physical causes and then to monitor any variation of mechanical properties.

To compute the PSD, we pre-processed hourly raw seismic traces from vertical-component seismometers, with: i) instrumental response deconvolution, demeaning and detrending; ii) clipping (high-amplitude removal by setting a maximum threshold equal to four-times the standard deviation). Then we computed PSD using Welch's estimate (Solomon, 1991) between 1 and 50 Hz (with Tukey windowing, 10% overlapping and 4096 points for discrete Fourier transform and then hourly-averaging and normalization by the hourly maximum). We then obtained hourly-normalized spectrograms, containing the relative weight of each frequency. We selected automatically significant and sharp peaks of the spectrum by using different threshold values for local maxima picking (minimum of peak frequency at 10 Hz, minimum of inter-peak distance at 4 Hz, maximum of width of 8 Hz, minimum of peak height at 0.2 and minimum of prominence at 0.3 for normalized spectra). We selected only frequency peaks above 10 Hz in order to prevent any source effects, since specific peaks of the rock glacier are assumed to be above this limit (see Figure 2).

For the Laurichard site, we used seismic traces of another station located in a stable area at Lautaret pass (see Figure 1b), named OGSA (RESIF, 1995). Since OGSA is considered as a reference station, we could compare spectral contents with the reference one, to evaluate the specific frequency peaks of the Laurichard rock glacier (see Figure 2 and Fig. 19 in Appendix C). In this way, we ensured that those picked frequencies are related to the modal signature of the rock glacier. Since no sensor was settled out of the rock glacier in Gugla site, we have not applied this method for this site.

We also applied the same method for earthquakes signals, but the results appear less clear than those from ambient noise (but shown and discussed in Appendix B).

3.2 Resonance frequency monitoring of Laurichard rock glacier

The spectrograms of Power Spectral Density (PSD), normalized every hour between 1 and 50 Hz, are shown for the two seismometers C00 and C05 in Figure 3. Several peaks of PSD appear and vary along time.

Among potential sources affecting the spectral content of seismic records, we aimed at selecting only natural resonance modes of the rock glacier structure. For example, we observed a very stable narrow peak of PSD at 23 Hz for both seismometers. This mode lights up mainly during summertime and in the daytime, although it remains visible during winter and in the night-time, but with significantly lower amplitude. Since this frequency peak is fully stable over time, we interpret its origin as either hydrological or anthropogenic. It may be generated either by groundwater flow within the rock glacier (Roeoesli et al., 2016), or by a pressure pipe located 400 m downstream or from road traffic coupled with a tunnel near the

Lautaret pass (see Figure 1). This frequency peak is also visible on spectrograms of station OGSA (see black arrow in Figure 2d) located at Col du Lautaret on a stable site, suggesting a potential anthropogenic source. The spectral content of these recordings exhibits the same peak at 23-24 Hz (see red curve in Figure 2d), implying it is not directly related to the rock glacier resonance. Then this frequency peak is hereafter excluded from the analysis.

The spectral content of seismic recordings can be affected by temporal variations of ambient seismic noise sources. For the two sites, these sources are assumed to originate from stable human activities located in the nearby valley and from weathering, but they could also be partly related to hydrological processes via melting water in spring and summer time. This source variability has to be addressed, in order to eliminate any spurious interpretation of actual changes in elastic properties. We then compare raw and normalized spectrograms of the reference station OGSA over one year (see Fig. 19 in Appendix C) to track any variation of the spectrum content which would prevent further comparison of frequency peaks observed on the rock glacier over time. No significant temporal changes of PSD appears within the illuminated spectrum of this stable station located near Laurichard rock glacier. Another obvious fact to highlight is that frequencies which were picked from ambient noise are also often visible when earthquakes signals are considered (see Appendix B). These two observations strengthen the direct link between these frequency peaks and rock glacier resonance.

Other spurious effects of artificial or non-specific sources affecting PSD are known: atmospheric effects (local structure or vegetation coupled with wind (Johnson et al., 2019)), loss of sensor coupling or water filling of the shelter of the sensor during melt out (Carmichael, 2019). However, these sources are not present at Laurichard rock glacier: for all sites the seismometers are well-coupled on flat and stable boulders, ensuring a good rock-to-sensor coupling. Each of them is sheltered by a plastic tube covered by a waterproof tarp, in order to prevent any influence of rain, wind and snow. During site visits, no water in the settlement was observed.

For the C00 seismometer, we observe a main peak of PSD between 15 and 20 Hz interpreted as the fundamental mode of the nearby area of the rock glacier (Figure 3a). The temporal evolution of this mode shows a seasonal cycle, characterized by higher frequencies during winters and lower frequencies during summers. A sudden drop of frequency occurs at the time when melting processes occur (blue boxes on Figure 3). Comparing the two winter periods, the maximum frequency is lower in 2019 (around 17 Hz) than in 2018 (around 19 Hz), while it remains constant around 15 Hz for the two recorded summers.

For sensor C05, we can follow the same peak considered as the fundamental mode of the corresponding area, with a similar seasonal cycle (Figure 3b). Again, the fundamental frequency increases during winter, and drops during melting periods and summer time. Compared to the C00 case, the amplitude of this seasonal variation is much higher: even if the frequency value in summer is similar (around 15 Hz), the winter one reaches a higher value (around 30 Hz). The maximum value is also higher in 2018 (35 Hz) than in 2019 (30 Hz).

3.3 Resonance frequency monitoring of Gugla rock glacier

We applied the same spectral analysis for the Gugla site. From the hourly normalized PSD of seismic noise recorded on the rock glacier (sensor C2), we observed two resonance frequencies evolving with time (Figure 4). At relatively high frequencies, a second mode is well measured, because the mean noise level is higher in Gugla than in Laurichard, where only the fundamental mode is observed.

As for Laurichard site, these frequencies present seasonal oscillations: they increase progressively to peak at cold winter periods, whereas they drop when melting processes occur at spring and summer time (blue boxes in Figure 4). The fundamental mode varies from 15 Hz in summertime to around 21 Hz in wintertime, whereas the second mode oscillates from 27 Hz to 40 Hz.

Again, the resonance frequency of the fundamental mode shows an inter-annual variability: in winter 2017 the maximum value is lower (around 20 Hz) than the peaks of the two other winters (around 24 Hz).

4 Mechanical modelling

4.1 Methodology

Using a finite-element method, we model rock glaciers as vibrating structures embedded in the bedrock. We then study the sensitivity of the modal response of this model to ambient seismic noise as a function of its elastic properties.

Elastic features can be determined as a function of compressional V_p and shear V_s seismic wave velocities, together with the density ρ. Therefore we evaluate seismic velocities along depth thanks to active seismic investigations complemented by Ground Penetrating Radar (GPR) surveys in order to obtain a 1D $[V_p(z), V_s(z), \rho(z)]$ profile describing the medium near the seismometer of interest. This first model is considered as a reference model since it has been built during unfrozen summer periods. In addition, we consider the effect of freezing-thawing processes on the elastic model using a poroelastic approach that enables to quantitatively evaluate elastic parameter changes due to the freezing. Modal analysis is then performed with Comsol software[1], in order to compute synthetic resonance frequencies that can be compared with the observed ones.

4.2 Reference model from geophysical investigations

Since one decade, numerous experiments have been devoted to geophysical characterization of rock glaciers (Maurer and Hauck, 2007; Kneisel et al., 2008; Haeberli et al., 2010) in order to constrain site modeling and better understand subsurface physical processes involved in their deformation. Among available geophysical methods, seismic refraction tomography (SRT), Ground Penetrating Radar (GPR) and Electrical Resistivity Tomography (ERT) have provided promising results. In alpine permafrost regions, the high heterogeneity of the subsurface together with cost-intensive and risky field conditions make

[1] COMSOL Multiphysics® v. 5.4, www.comsol.com, ComsolLab, Stockholm, Sweden.

geophysics challenging. However, combining the geophysical methods listed above give useful information in a view of imaging and modeling the subsurface.

4.2.1 Laurichard rock glacier model

4.2.1.1 Ground Penetrating Radar survey

We performed a Ground Penetrating Radar (GPR) campaign at the end of June 2019 to better assess the geometry and the internal structure of the Laurichard rock glacier. It is composed of (i) a common-offset longitudinal profile starting in the middle of the rock glacier and stopping near the front, following the main flow line and (ii) a common-offset transversal profile crossing over the rock glacier width, approximately following the C01-C04 seismometers line discussed afterwards (Figure 1a). The method and resulting figures are shown in Appendix D and Figure 5.

Both GPR images show relatively continuous reflectivity within the rock glacier, particularly along the longitudinal direction (Figure 5(2a)), indicating a stratification of the deposits. The use of low frequency antenna certainly naturally homogenized the heterogeneity of rock glaciers, as witnessed by the quasi-absence of diffraction. The thickness of the glacier varies weakly along the longitudinal direction, ranging from 28 m upstream to 10 m downstream. More abrupt variations are detected in the transverse direction (Figure 5(2b)), from a few meters to 20 m at the center and the eastern part. It must be noted that the first few meters of the rock glacier cannot be resolved, due to the antennas configuration with a large source-receiver offset and the large wavelength (about 4.8 m).

As a conclusion, the bedrock interface depth is well constrained by GPR results, combining longitudinal and transversal profiles. In the lower part of the rock glacier near the front, the bedrock is estimated at around 10 m depth. But the transversal profile also reveals heterogeneities over the seismic array. In the western part (C05) the rock glacier seems thinner than in the eastern part (C00), according to the bedrock depth estimation based on contour line interpolation on both sides of the rock glacier. By Digital Elevation Model (DEM) difference between surface and bedrock (see 0), we then more precisely estimated the interface depth (14 m for C00 and 8 m for C05, see Figure 8(b)).

4.2.1.2 Seismic tomography

A seismic refraction/tomography survey has been performed in July 2019. This experiment consists of active seismic recordings with controlled sources, in order to determine the P-wave velocity distribution along a 2D line. The profile is roughly located along the C1-C4 line, near the center of the seismic array (Figure 1a). The method and resulting figure are shown in Appendix D and Figure 6. The result shows 2D variations with some degree of layering in the velocity distribution. The interface between the rock glacier and the bedrock might be marked by the large interface separating a material with velocities lower than 2000 m/s with a layer showing a large velocity about 3000 m/s (Fig. 6). Its thickness varies from 10 m to 20 m, which is consistent with GPR results (Figure 5(2)). To overcome the smoothing effect of seismic tomography, data

have also been processed using seismic refraction with two opposite large-offset shots. This approach highlights a layered structure of the medium, with different slopes and particularly an interface located around a depth of 4 m, which probably separates the active layer from the permafrost one. Therefore, we can assume an active layer from the surface to 4 m depth, corresponding to the maximal depth where the medium is totally thawed in summertime.

4.2.1.3 Multichannel Analysis of Surface Waves (MASW)

In order to better understand the seismic wavefield and constrain the S-wave velocity distribution at the site, we analyzed the surface Rayleigh waves, which dominate the vertical seismic records used in the tomography. The method and resulting figure are shown in Appendix D and Figure 7.

The Vs profiles displayed in Figure 7b shows a large variability but the best fitting models all converge towards an interface located at 5 m depth with a superficial velocity of 155 m/s followed by a linear increase of velocity reaching 750 m/s at a depth of 7 m. The best model also shows another deeper interface, at 15 m depth, which could be the bedrock interface, despite the low resolution at this depth.

From all these geophysical surveys, a tentative 1D seismic velocity model was built for each seismometer (C00 and C05), as the reference unfrozen model. Its values have been well constrained by seismic refraction, whereas bedrock interface depth has been constrained by GPR results, together with interpolated DEM differences (Figure 8).

4.2.2 Gugla rock glacier model

To establish a reference model of the Gugla rock glacier, we use seismic velocities that have already been constrained by a seismic refraction survey (Fig. 1b) performed in July 2017 during a summer and dry period (Figure 9). All values for Vp and Vs profiles have been already presented in a previous study (Guillemot et al., 2020). We also assume a density profile that progressively increases, from $\rho = 2000\ kg/m^3$ at the surface to $\rho = 2800\ kg/m^3$ at the bedrock.

Moreover, we estimate the bedrock at 23 m depth, in accordance with observations provided by boreholes located near the seismometer of interest (borehole F2, (CREALP, 2015)).

4.3 Freezing modeling from poroelastic approach

4.3.1 Methods and results

In order to mimic the freeze-thawing effect on resonance frequencies, the associated variations of elastic properties of the material have to be constrained by seismic velocity changes. A winter model is required to be compared to the summer one. For the transition from summer to winter, an increase of P- and S-wave velocities during winter is expected, in accordance with laboratory and numerical experiments (Timur, 1968; Carcione and Seriani, 1998; Carcione et al., 2010). Indeed, both

bulk and shear moduli of the effective medium increase during freezing, generating a global stiffening of the upper part of the rock glacier subject to the seasonal thermal forcing.

In order to quantify the evolution of these elastic parameters with freezing, we use a poroelastic approach assuming a three-phase model: a rock glacier is considered as a porous material composed of pores embedded into a granular rocky matrix. We then address the sensitivity of elastic parameters to the proportion of liquid water and ice filling the pores, for several porosity values. Since the wavelength of seismic waves is much greater than the size of the pores, this homogenization approach holds. As did Carcione and Seriani (1998), we use a Biot-Gassmann type three-phases model that considers two solid matrices (rock and ice) and a fluid one (liquid water). Since the contribution of air proportion within the pore is negligible on the shear modulus, which mostly determines the fundamental vibrating mode, we omit the air phase for the sake of simplicity.

We apply the following methodology for the three cases (Gugla C2, Laurichard C00 and C05). Several parameters are required to completely describe the poroelastic state of a rock glacier: bulk and shear moduli of the respective pure phases, the averaged density, the porosity and the water saturation.

For the summer state of the rock glacier, we evaluate these parameters indirectly. The density ρ is fixed at realistic values ($\rho = 1800\ kg/m^3$ for the first two meters, $\rho = 2000\ kg/m^3$ for the deeper part of the rock glacier, and $\rho = 2650\ kg/m^3$ for the bedrock, (Hausmann et al., 2012)), as well as the porosity profile (see references in paragraph 4.3.2). The water saturation s is assumed at $s = 0$ for the first two meters, and $s = 0.2$ deeper, in consistency with visual observations and qualitative features performed from boreholes in summer (CREALP, 2016). Respective bulk and shear moduli of the pure phases (ice and water) are fixed from the example of Berea sandstone ((Carcione and Seriani, 1998), Table 2). The bulk and shear moduli of the dry solid matrix have been obtained from the inversion of velocities using a Biot-Gassmann poroelastic model with two phases (solid matrix and water). For this inversion step, we use water saturation, porosity and seismic velocity profiles (V_p, V_s) deduced from seismic refraction geophysics performed in summer (see 0 for Laurichard and 0 for Gugla). The outputs of this inversion step are the elastic moduli of the solid matrix, assumed constant along seasons, and describing the elastic behaviour of the rock glacier without neither water saturation nor seasonal freezing. The profile of all the parameters of this summer model are shown in Figure 10(b,c,d,e) in red curves.

For the winter state of the rock glacier, we keep unchanged the porosity and elastic parameters of the three phases (water, ice, and solid matrix), but we assume the pores are fully filled by ice (water saturation equals to zero) from the surface to the maximum depth where seasonal freezing acts, also called Zero Annual Amplitude (ZAA) depth. ZAA is estimated to approximately 8 m depth from thermal investigations in Gugla ((CREALP, 2016)), and extrapolated as well to Laurichard. The averaged density is computed by averaging the density of each phase, weighted by their respective volumetric ratio.

The seismic velocity profiles (V_p, V_s) for a totally frozen state are then computed by applying the 3-phases poroelastic model. For this step, the input parameters are the porosity and the density, together with bulk and shear moduli of each phase (water, ice and solid matrix). These elastic parameters are homogeneized according to Carcione and Seriani, 1998, and then equations of wave propagation are solved in order to obtain fast P-wave and S-wave velocities as modeled by Leclaire et al., 1994. Results of the evolution of these velocities with respect to ice/water ratio filling the pores are shown in Figure 11 for the

example of Laurichard (sensor C00). Hence we deduce the values for a frozen state of the rock glacier with pores totally filled by ice between the surface and ZAA. We acknowledge that this is a strong assumption for the winter state, and that other models may also explain our observations. The profiles of all the parameters of this winter model are shown in Figure 10 (b,c,d,e) with blue curves.

With these two models in summer (minimum of freezing) and winter (maximum of freezing), we can also model the transition between them. Although the freezing process (from summer to winter) is poorly constrained, due to liquid water infiltration and complex thermal forcing, the thawing process (from winter to summer) appears easier to model, assuming a temporal evolution of thawing mainly controlled by thermal heat wave propagating from the surface to the ZAA depth. Hence, we build an intermediate state of the rock glacier by introducing another parameter, called "maximum depth of thawing" (see Figure 10a). This parameter establishes an interface between the unfrozen state (as the summer model) above it, and the frozen state (total pore filling by ice) below it. Hence, this maximum depth of thawing evolves from the surface to the ZAA with 1 m increments, reporting as many intermediate models. The profile of the parameters of an example of intermediate model are shown in Figure 10 (b,c,d,e) in purple dashed curves.

Finally, we compute the modal response (explained below in section 4.4) of the corresponding vibrating structure of all these models (summer, intermediate and winter), modeling a value of resonance frequency depending of the freezing state of the rock glacier.

4.3.2 Influence of the porosity

Defined as the ratio between pore volume and total volume, the porosity ϕ of the rock glacier is one of the key parameters influencing the mechanical modeling. Our three-phase poroelastic model actually considers the filling of pores by two phases (ice and water), together with interaction between ice and rocky debris matrices that strongly depends on porosity. In the absence of any *in-situ* information, we assume a model of spherical particles stacking (Rice, 1993), decreasing with depth due to compaction ($\phi = 0.35$ for sublayers from the surface to 2 m depth and $\phi = 0.25$ elsewhere below, for both sites). In order to quantitatively assess the sensitivity of our results to porosity, we also apply the mechanical modeling to other profiles considering extreme values (low limit: $\phi = 0.2$ in the active layer and $\phi = 0.15$ elsewhere, and high limit for this rock glacier lithology (Arenson and Springman, 2005): $\phi = 0.6$ everywhere). As expected, the higher porosity values, the higher the influence of the ice pore filling on the elastic parameters, and thus the higher the variation of modeled resonance frequencies. Then in the following results presented below, errorbars correspond to the sensitivity on the porosity (low limit for low porosity, high limit for high porosity, see values in transparence in Figure 13).

4.4 Modal analysis and frequency response of the rock glacier

We build a mechanical model on Comsol software based on the finite-element method, in order to numerically compute its resonance frequencies and modal response (see Appendix D for details). The rock glacier is modeled as a 2-D rectangular vibrating structure embedded in the bedrock (or a stable bottom layer). The height H of the structure is fixed at the

corresponding depth of bedrock (see Figure 8 for Laurichard and Figure 9 for Gugla). The model is vertically sub-sampled into 2 m thick sublayers, with elastic parameters interpolated from averaged values of seismic tomography results, and with a usual isotropic attenuation factor of 1% (Bonnefoy-Claudet et al., 2006). Depending on the direction of the model (longitudinal or transversal), the width of the structure varies in accordance with the whole rock glacier size (several tens of meters), permitting an infinity of vibration modes. Based on a polarization analysis from ambient noise between 1 and 50 Hz in the Gugla rock glacier in summer 2016, we observed that the wavefield of rock glaciers is mostly polarized in a parallel to the slope direction. Similar to the fundamental mode of an unstable rock mass (Burjánek et al., 2012) and avalanche glaciers (Preiswerk et al., 2019), the measured polarization is almost linear (ellipticity lower than 0.15) and thus corresponds best to shear modes. We then computed the Frequency Response Function (FRF) (Fu and He, 2001) on the whole length (several hundreds of meters for both cases) of the rock glacier, in order to obtain its resonance frequencies corresponding to vibration modes of the mechanical structure. For this step, we simulated several seismic sources located at the base of the vibrating structure (see red crosses in Figure 12a), producing harmonic forces from 1 to 50 Hz in all directions. The amplitude of this modeled seismic noise is not frequency-dependent, while it decreases generally with frequency on the field, showing probably the excitation of other modes than the recorded ones (especially in Laurichard). However, after checking that resonance frequencies obtained from FRF with high amplitude of vertical displacement (Figure 12b) would not be modified, we reduced the width of the model to 5 m by applying symmetrical conditions at the boundaries perpendicular to the slope (Figure 12c), in order to facilitate the following parametric modal analysis.

4.5 Comparison between observed and modeled resonance frequencies

We show the results from the modal analysis on Comsol software for only the observed modes with a vertical component (first mode for Laurichard, the two first modes for Gugla) in Figure 13. Nine mechanical models have been tested, corresponding to different steps of thawing with elastic parameters selected as described in 4.3. Thus, we present modeled resonance frequencies with respect to the maximal depth of thawing, from the surface to 8 m depth (Figure 13). As expected, resonance frequencies of these modes match the frequency band of measurements below 50 Hz and generally decrease with thawing. We compare them to the maximum (in winter) and minimum (in summer) values observed on all sites (depicted in squares in Figure 13, which are values from Figure 3 for Laurichard and Figure 4 for Gugla). The modeled resonance frequencies fit well the observed ones, considering error bars related to porosity uncertainties (see 4.3.2). Regarding the fundamental mode (mode 0), the resonance frequency is of the same order of magnitude (between 15 and 20 Hz) for both sites (i.e. Gugla and Laurichard). Focusing on the two sensor locations in Laurichard, a stronger effect of freezing is observed for C05 than for C00 model. Hence, the bedrock is shallower under C05 than under C00 (8 m and 14 m, respectively), highlighting the role of the height of the local vibrating structure on seasonal amplitudes. In general, these numerical results explain well the seasonal variations of observed resonance frequencies, assuming a thawing process from the surface to 8 m depth between winter and summer.

5 Discussion

From the results of mechanical simulation on both Laurichard and Gugla rock glaciers, we draw several conclusions:

- The vibrating modes of rock glaciers can be tracked from spectrograms of seismic ambient noise. The resonance frequencies from the mechanical modeling fit well the measured ones (between 15 Hz and 20 Hz in summer for both sites) within experimental errorbars. This validates our methodology based on rock glacier modeling as a vibrating structure, at least for the first mode;
- Monitoring these resonance frequencies along time allows to observe seasonal evolution: all the modes show a progressive increase of the resonance frequencies during winter, followed by a sudden drop at the onset of melting periods in spring and lower values during summers.
- According to the poroelastic approach used to model the effect of freezing on seismic velocities, this variation is qualitatively well explained by freeze-thawing processes. Indeed, the annual heat wave propagates into the surface layers of the rock glacier (Cicoira et al., 2019; CREALP, 2016), causing a change of frozen material content within the porous medium, and thus a large variation of elastic properties due to this thermo-mechanical forcing. For both sites and sensor locations, this modeled mechanical forcing provides a good estimation of the observed frequency seasonal variations, quantitatively. The modeled changes of elastic parameters (bulk and shear moduli increasing through seismic velocities) involved for Gugla rock glacier (Guillemot et al., 2020) have thus been improved by this complementary method based on a more complete description of poroelasticity, though other models may also explain our observations.
- By tracking resonance frequencies in long term, we are able to detect an inter-annual variability. Interestingly, the freezing process appears to correlate with annual minimum of resonance frequency: as an example, in 2019 in Laurichard, the winter resonance frequency was lower than in 2018, indicating a lower rigidity of the medium due to reduced frozen material content. The winter was actually colder in 2018 than in 2019: from a meteorological station near the col du Lautaret (1 km from Laurichard), the mean air temperature during snow cover T_{winter} was lower in 2018 ($T_{winter}(2018) = -2.07\,°C$) than in 2019 ($T_{winter}(2019) = -0.50\,°C$). The intensity of freezing is generally estimated from Freezing Degrees Day (FDD), defined as a time cumulative sum of each ground surface temperature below 0°C recorded during one wintertime. According to an earlier and longer snow cover period in 2019 than 2018 that insulates the ground from the air forcing, the internal freezing of the rock glacier was less intense in 2019 ($FFD(2019) = -322\,°C.day$) than in 2018 $FFD(2018) = -451\,°C.day$). Similarly for the Gugla site, the winter resonance frequency was significantly lower in 2017 (19 Hz) than in the others years (around 23 Hz). Despite a comparable mean air temperature between 2016 and 2017, the earlier and longer snow cover period in 2017 promoted a lower freezing of the internal layers. We finally conclude that resonance frequency in wintertime indicates well the intensity of freeze-thawing effects on the rock glacier.
- Despite a high level of heterogeneities within rock glaciers, low-frequency GPR results allow to better constrain the bedrock interface depth. For Laurichard, the mean value was estimated at 10 m (+/-50% due to the underneath slope).

According to field observations and DEM interpolation, we fixed this value at 14 m for C00 model, and 8 m for C05 model. This unique difference between the two locations explains very well the observed difference of seasonal resonance frequency amplitude (Figure 3): the shallower the bedrock interface, the larger this amplitude. In addition to active seismology allowing to perform 2D seismic velocity tomographies, low-frequency GPR results provide valuable information about internal structure of the surveyed rock glaciers, reinforcing the benefits of geophysical investigations in combination with passive seismology in rock glaciers.

The relation between ground surface temperature and resonance frequencies is plotted in Figure 14 (for Laurichard C00 case). It reveals an annually repeated pattern showing a hysteretic behavior. This relation suggests several phases along the year (indicated with colors and numbers in Figure 14b), depending on the state of freezing of the rock glacier: 1) unfrozen phase (late summer and autumn), when temperature is varying above 0°C while resonance frequency stays at its lowest level ; 2) shallow freezing phase (late autumn and early winter), when temperature decreases below 0°C (with possible significant drops depending on the presence of snow cover insulating the medium or not), while resonance frequency starts to increase ; 3) deep freezing phase (late winter), when temperature is stabilized due to insulation by permanent snow cover, while the freezing front propagates deeper, increasing the resonance frequency ; 4) Shallow thawing phase (early spring), when temperature reaches 0°C and stay during a zero-curtain period, indicating phase change together with melting water percolating into the active layer and sometimes re-freezing, while resonance frequency drops due to thawing of surface layers ; 5) deep thawing phase (late spring and early summer), when the heat wave propagates deeper in the medium, keeping the decrease in resonance frequency up.

In comparison with other passive seismic methods, as relative seismic velocity variations computed from ambient noise correlation that has already been applied in Gugla (Guillemot et al., 2020), the spectral analysis of seismic noise (presented here) is easier to process. Combined with the modal analysis of a mechanical model of the site, the spectral content accurately records the seasonal freeze-thawing cycle, reinforcing observations from ambient noise correlation (Guillemot et al., 2020). Beyond these similarities, the main difference between these two methods is their depth sensitivity. Frequency resonance focuses on isolated frequencies, whereas ambient noise correlations exploits the whole spectrum, thereby surveying a larger range of depths. To quantify this difference between the two methods, we computed sensitivity kernels for each one. It consists in evaluating the changes (of frequency or dV/V) after a 50% increase of seismic velocities V_p and V_s for a 0.5 m thick sublayer along the depth of the modeled rock glacier. All the parameters are those of the summer models (for Gugla in Figure 9, for Laurichard C00 and C05 in Figure 8(c)), and kernels have been computed for all these three sites. These results are presented in Fig. 15: 1) for ambient noise correlation method: we compute the dispersion curves of the Rayleigh waves using the Geopsy package (Wathelet et al., 2004). The theoretical relative velocity changes (dV/V) are computed by measuring the difference between the modified dispersion curve with the reference one at each frequency ; 2) for modal analysis method, the resonance frequency of the fundamental mode of the vibrating structure modeling the rock glacier is obtained using Comsol software.

For both methods, their kernels have been normalized by their maximum value along depth, allowing an estimation of the depth where the sensitivity of the method is the highest. The results are shown in Figure 15 for Laurichard C00 sensor, while other sites are not presented but yield similar results. For all sites, modal analysis is most sensitive at a relatively shallow depth (5 m for Gugla, 4 m for Laurichard C00, 3 m for Laurichard C05) in the active layer, whereas ambient noise correlation has a broader sensitivity, including shallower and deeper layers depending on the frequency band (the lower the frequency, the deeper the penetration). Therefore, the modal analysis permits to easily evaluate the state of freezing of rock glaciers, surveying mostly the depth range between 2 m and 8 m, including the active layer (< 5 m), while ambient noise correlation at low frequencies allows the same monitoring over a broader range of depths but requires additional data processing. Furthermore, ambient noise correlation may provide less stable results at high frequencies (up to 14 Hz, for the Gugla study (Guillemot et al., 2020)), preventing any interpretation of the chaotic results due to the lack of high frequency noise in the cross-correlation at large inter-sensor distance. Hence, the sensitivity of the different methods depends also on the nature of the ambient noise wavefield together with the sensor network setup. According to the site and its instrumentation, the two passive seismic methods may be combined to obtain stable results along the whole depth of the rock glacier. As many other geophysical techniques, the present study is therefore to be considered as one element among other parts of a global monitoring strategy.

6 Conclusion

For two rock glaciers, we monitored the resonance frequencies of vibrating modes during several years thanks to continuous seismic noise measurements. These frequencies show seasonal variations, related with changes in elastic properties of the structure underneath the recording sensor, due to freeze-thawing effects. Assuming vibrating systems, we performed a 2D mechanical modeling of rock glaciers, which fit well the recorded resonance frequencies. By estimating elastic properties derived from active seismic measurements, we have reproduced the observed lowest values in summer, when active layer is totally thawed. By quantitatively modeling the increase of rigidity due to freezing in wintertime using a poroelastic approach, we have reproduced the observed higher values in winter due to maximum freezing in active layer. These results highlight the sensitivity of resonance frequency on seasonal freeze-thawing cycles.

The results of this modal analysis have been obtained from a model constrained by geophysical investigations, as Ground Penetrating Radar and seismic tomography surveys. This study shows that the two approaches (spectral analysis of seismic data, combined with GPR and seismic refraction) provide a consistent understanding of seasonal variations of rock glacier rigidity, mainly forced by the freezing effect of those porous media.

Among passive seismic methods on rock glaciers, the spectral analysis appears as an easy and effective monitoring tool of the active layer, which is subjected to significant seasonal changes. At greater depths and lower frequencies, the seismic data can be preferably processed using a pair of stations by computing ambient noise correlation. This can be useful to complement observations of resonance frequencies, in addition to bringing new insights into other processes occurring at greater depth,

such as groundwater or structural changes within rock glaciers. On the long term, seismic vibrations offer the possibility to monitor the effect of global warming on the permafrost degradation.

7 Acknowledgments

Seismic data of Laurichard rock glacier are available at the French RESIF seismological portal (http://dx.doi.org/10.15778/RESIF.1N2015). Seismic data of Gugla rock glacier are available upon request at CREALP. Some valuable information about the geophysical campaign, data from boreholes and their interpretation were shared with permission from CREALP (see weblink in references). We are particularly grateful to Benjamin Vial and Mickaël Langlais (ISTerre - SIG), Guillaume Favre-Bulle (CREALP) and Ludwig Haas (Wallis canton) and the geological department of Wallis for their invaluable assistance with fieldwork, site maintenance and seismic data retrieval of Gugla rock glacier. This work is supported by the OSUG@2020 Labex, the VOR-UGA program, the CNRS-INSU program, and the ANR LabCom GEO3iLab. For Laurichard site, one part of the research was partially supported by Lautaret Garden-UMS 3370 (Univ. Grenoble Alpes, CNRS, SAJF, 38000 Grenoble, France), member of AnaEE-France (ANR-11_INBS_0001AnaEE_Services, Investissement d'Avenir frame) and of the eLTER-Europe network (Univ. Grenoble Alpes, CNRS, LTSER Zone Atelier Alpes, 38000 Grenoble, France).

Appendix A: Time series of ground surface temperature (Laurichard rock glacier)

In Fig. 16 we show the time series of the measured ground surface temperature at several locations on and near the Laurichard rock glacier. These measurements help to date the snow cover periods with zero-curtain effect, together with freezing periods.

Appendix B: Frequency picking of earthquakes signals

In addition to spectral analysis from ambient noise, PSD of earthquakes signals emerging from noise have also been computed. For both sites, such signals have been sorted out from a catalog of earthquakes (magnitude M>2). For the Laurichard area, we used all earthquakes recorded by the Sismalp catalog[2]. We thus applied the same processing than for noise (without any clipping) for the 60 s-long raw trace containing the signal of earthquakes, and finally track resonance frequencies of these quakes by maxima picking (Figure 2). For the Laurichard site, we used seismic traces of another station located in a stable area at Lautaret pass (see Figure 1), named OGSA (RESIF, 1995). Since OGSA is considered as a reference station, we computed a site-to-reference spectral content to evaluate the specific frequency peaks of the Laurichard rock glacier (see Figure 2). In this way, we ensured that those picked frequencies are related to the modal signature of the rock glacier. Overall, this

[2] https://sismalp.osug.fr/evenements

method of spectral analysis allows comparing the spectral response of the structure to low (seismic noise) and higher (earthquakes) levels of excitation.

The resonance frequencies estimated using earthquake signals (white dots on Fig. 18) appear similar to the ones estimated from noise for C00 seismometer. However, there are more discrepancies for sensor C05. For this sensor, the peak frequencies determined from seismic signals show more fluctuations than when picking resonance frequencies from PSD of seismic noise.

Appendix C: Ambient noise source variability over one year

In order to address the effects of seasonal changes of seismic sources, we compare raw and normalized spectrograms of seismic recordings acquired both on rock glaciers and on a stable nearby site. Here we present the results for the OGSA station (RESIF, 1995), located in Lautaret pass (2 km from Laurichard rock glacier) in 2019 (see Fig. 19). From these raw spectrograms, we observe a seasonal variability of noise level, suggesting a seasonal variability of the noise sources (higher in summer than in winter, probably due to intensified road traffic and fluvial processes in summer). From the normalized spectrograms, we notice that no significant changes of frequency peaks appear within the illuminated spectrum of interest (10-40 Hz). Since the OGSA station (stable reference) is located close to the Laurichard rock glacier, we assume that ambient noise sources are roughly the same for both sites. Therefore we conclude that seasonal variability of frequency peaks recorded on the rock glacier between 15 and 40 Hz (see Figure 3) is not much influenced by seismic source changes, but rather linked to specific resonance of the rock glacier structure.

Appendix D: Geophysical surveys in Laurichard rock glacier

Ground Penetrating Radar survey

Preliminary tests have demonstrated the ability of the 25 MHz Rough Terrain Antennas (RTA) to follow the continuity of the reflectors throughout the glacier, despite lower resolution (wavelength about 4.8 m). The 100 MHz antennas actually experienced penetration problems, presumably related to the presence of heterogeneities equivalent in size to the wavelength (about 1.2 m). In addition, a Common Middle Point (CMP) survey was performed along the western part of the transverse profile using unshielded bi-static 100 MHz antennas, in order to assess locally the electromagnetic wave velocity distribution within the glacier. Fig. 5(1a) shows the CMP data after trace by trace amplitude normalization and gain amplification using a dynamic automatic gain control computed on a 100 ns time window. After the direct air and ground waves, numerous events exhibiting a hyperbola shape can be recognized from 40 ns to 225 ns in the CMP data. These hyperbolas have been analyzed considering a semblance analysis (Fig. 5(1b)), which yields the stacking velocity versus propagation time where a semblance is maximum. The picked maximum of the velocity distribution shows variations ranging from 14 cm/ns to 11 cm/ns with a mean velocity of 12 cm/ns. As these variations are measured on apparent velocities, the real variations are larger when layers are considered. They can be qualitatively interpreted in terms of an increase of air (velocity of 30 cm/ns) and ice (velocity of 17 cm/ns) content when velocity is large, and an increase of water content (velocity of 3.33 cm/ns) when

velocity drops. Considering a mean velocity of 12 cm/ns, the 100 MHz CMP analysis penetrates to a depth of 13.5 m and the increase of velocity arriving nearby 110 ns corresponds to a depth around 6 m.

Figure 5(2) shows both common-offset profiles acquired using the 25 MHz antennas after they were processed using: i) time-zero source correction, ii) normal-moveout correction as source and receivers are separated by an offset of 6.2 m for these antennas, iii) static corrections for topography iv) migration and v) time to depth conversion. The later processing steps have been performed considering a mean velocity of 12 cm/ns, a value deduced from the CMP analysis (Fig. 5(1b)).

Seismic tomography

A seismic refraction/tomography survey has been performed in July 2019. This experiment consists of active seismic recordings with controlled sources, in order to determine the P-wave velocity distribution along a 2D line. The profile composed of 24 geophones (4.5 Hz) deployed every 3 m is roughly located along the C1-C4 line, near the center of the seismic array (Figure 1a). The first arrival time picking of the 8 shots have been inverted using a Simultaneous Iterative Reconstruction Technique (SIRT, (Demanet., 2000)) in order to obtain the P-wave velocity distribution along the profile (Figure 6). From an initial model with a uniform velocity of 3000 m/s (340 m/s in the air), 25 iterations were performed to reconstruct observations ($RMS\ misfit = 8\ ms$).

Multichannel Analysis of Surface Waves (MASW)

In order to better understand the seismic wavefield and constrain the S-wave velocity distribution at the site, we analyzed the surface Rayleigh waves, which dominate the vertical seismic records used in the tomography. For this, we used a far offset shot and computed the semblance map of the velocity and frequency of the waves dominating the seismic record (Figure 7a), obtained using the Geopsy package (Wathelet et al., 2004).

The semblance map shows several continuous modes, while the fundamental dispersion curve was picked from 14 Hz to 30 Hz, as indicated by the black line. The presence of several other modes is due to the presence of strong contrasts within the rock glacier and at the interface between the rock glacier and the bedrock. The dispersion curve was inverted using the Geopsy/dinver package (Wathelet et al., 2004), where a global neighborhood algorithm optimization method is implemented. The model was parametrized using four layers, the top three searching for linear velocity gradients in each layer. With the available frequency range and the velocity distribution, the resolution at large depths (> 15 m) is rather poor.

Appendix D: Modal analysis using finite element method

The finite-element method aims to numerically estimate the resonance frequencies of a vibrating structure, by solving the Newton's second law for the displacement of the considered degrees of freedom $V(t)$ (Bathe, 2006). Assuming free-equilibrium and no attenuation, the equation is:

$$[M]\{\ddot{V}(t)\} + [K]\{V(t)\} = \{0\} \quad (1)$$

where $[M]$ is the global mass, $[K]$ is the global stiffness matrix, and the dot means time derivative. Both $[M]$ and $[K]$ matrices are obtained by correctly assembling the respective element matrices, in accordance with finite-element method (Bathe, 2006). As a result, the solutions of equation (1) have to be of the form

$$\{V(t)\} = \{\psi\}\sin[\omega(t - t_0)] \quad (2)$$

where $\{\psi\}$ refers to a vector of order n, ω is a constant identified to the corresponding pulsation of the vibrating mode $\{\psi\}$, and t and t_0 are respectively the time variable and an arbitrary time constant.

Equations (1) and (2) provide the generalized eigen problem:

$$[M^{-1}K]\{\psi_j\} = \omega_j^2\{\psi_j\} \quad (3)$$

By solving this linear system, we can deduce the modal parameters: the n eigenvalues ω_j^2 (with $0 \leq \omega_1^2 \leq \omega_2^2 \leq \cdots \leq \omega_n^2$) and the corresponding eigenvectors $\{\psi_j\}$. The eigenvector $\{\psi_j\}$ is called the *j*-th modal shape vector that vibrates at the frequency $f_j = \omega_j/(2\pi)$.

References

Amitrano, D., Arattano, M., Chiarle, M., Mortara, G., Occhiena, C., Pirulli, M., Scavia, C., 2010. Microseismic activity analysis for the study of the rupture mechanisms in unstable rock masses. Natural Hazards and Earth System Sciences 10, 831–841. https://doi.org/10.5194/nhess-10-831-2010

Arenson, L.U., Kääb, A., O'Sullivan, A., 2016. Detection and Analysis of Ground Deformation in Permafrost Environments. Permafrost and Periglacial Processes 27, 339–351. https://doi.org/10.1002/ppp.1932

Arenson, L.U., Springman, S.M., 2005. Triaxial constant stress and constant strain rate tests on ice-rich permafrost samples. Can. Geotech. J. 42, 412–430. https://doi.org/10.1139/t04-111

Barsch, D., 1996. Rockglaciers: indicators for the present and former geoecology in high mountain environments. Springer, New York, NY.

Bathe, K.-J., 2006. Finite Element Procedures. Klaus-Jurgen Bathe.

Bodin, X., Krysiecki, J.-M., Schoeneich, P., Roux, O.L., Lorier, L., Echelard, T., Peyron, M., Walpersdorf, A., 2016. The 2006 Collapse of the Bérard Rock Glacier (Southern French Alps). Permafrost and Periglacial Processes 28, 209–223. https://doi.org/10.1002/ppp.1887

Bodin, X., Thibert, E., Fabre, D., Ribolini, A., Schoeneich, P., Francou, B., Reynaud, L., Fort, M., 2009. Two decades of responses (1986–2006) to climate by the Laurichard rock glacier, French Alps. Permafrost and Periglacial Processes 20, 331–344. https://doi.org/10.1002/ppp.665

Bodin, X., Thibert, E., Sanchez, O., Rabatel, A., Jaillet, S., 2018. Multi-Annual Kinematics of an Active Rock Glacier Quantified from Very High-Resolution DEMs: An Application-Case in the French Alps. Remote Sensing 10, 547. https://doi.org/10.3390/rs10040547

Bonnefoy-Claudet, S., Cotton, F., Bard, P.-Y., 2006. The nature of noise wavefield and its applications for site effects studies. Earth-Science Reviews 79, 205–227. https://doi.org/10.1016/j.earscirev.2006.07.004

Buchli, T., Kos, A., Limpach, P., Merz, K., Zhou, X., Springman, S.M., 2018. Kinematic investigations on the Furggwanghorn Rock Glacier, Switzerland. Permafrost and Periglacial Processes 29, 3–20. https://doi.org/10.1002/ppp.1968

Burjánek, J., Gassner-Stamm, G., Poggi, V., Moore, J.R., Fäh, D., 2010. Ambient vibration analysis of an unstable mountain slope. Geophys J Int 180, 820–828. https://doi.org/10.1111/j.1365-246X.2009.04451.x

Burjánek, J., Moore, J.R., Yugsi Molina, F.X., Fäh, D., 2012. Instrumental evidence of normal mode rock slope vibration. Geophys J Int 188, 559–569. https://doi.org/10.1111/j.1365-246X.2011.05272.x

Carcione, J.M., Morency, C., Santos, J.E., 2010. Computational poroelasticity — A review. GEOPHYSICS 75, 75A229-75A243. https://doi.org/10.1190/1.3474602

Carcione, J.M., Seriani, G., 1998. Seismic and ultrasonic velocities in permafrost. Geophysical Prospecting 46, 441–454. https://doi.org/10.1046/j.1365-2478.1998.1000333.x

Carmichael, J.D., 2019. Narrowband signals recorded near a moulin that are not moulin tremor: a cautionary short note. Annals of Glaciology 60, 231–237. https://doi.org/10.1017/aog.2019.23

Cicoira, A., Beutel, J., Faillettaz, J., Vieli, A., 2019. Water controls the seasonal rhythm of rock glacier flow. Earth and Planetary Science Letters 528, 115844. https://doi.org/10.1016/j.epsl.2019.115844

CREALP, 2016. Glacier rocheux de Gugla - Investigations 2015.

CREALP, 2015. Glacier rocheux de Gugla - Investigations 2014 - Calcul des volumes instables.

Delaloye, R., Morard, S., Barboux, C., Abbet, D., Gruber, V., Riedo, M., Gachet, S., 2012. Rapidly moving rock glaciers in Mattertal 11.

Delaloye, R., Perruchoud, E., Avian, M., Kaufmann, V., Bodin, X., Hausmann, H., Ikeda, A., Kääb, A., Kellerer-Pirklbauer, A., Krainer, K., Lambiel, C., Mihajlovic, D., Staub, B., Roer, I., Thibert, E., 2008. Recent interannual variations of rock glacier creep in the European Alps, in: Delaloye, R; Perruchoud, E; Avian, M; Kaufmann, V; Bodin, X; Hausmann, H; Ikeda, A; Kääb, A; Kellerer-Pirklbauer, A; Krainer, K; Lambiel, C; Mihajlovic, D; Staub, B; Roer, I; Thibert, E (2008). Recent Interannual Variations of Rock Glacier Creep in the European Alps. In: 9th International Conference on Permafrost, Fairbanks, Alaska, 29 June 2008 - 3 July 2008, 343-348. Presented at the 9th International Conference on Permafrost, University of Zurich, Fairbanks, Alaska, pp. 343–348. https://doi.org/info:doi/10.5167/uzh-7031

Demanet D., 2000. Tomographie 2D et 3D à partir de mesures géophysiques en surface et en forage. PhD thesis, University of Liège.

Duvillard, P.A., Revil, A., Qi, Y., Ahmed, A.S., Coperey, A., Ravanel, L., 2018. Three-Dimensional Electrical Conductivity and Induced Polarization Tomography of a Rock Glacier. Journal of Geophysical Research: Solid Earth 123, 9528–9554. https://doi.org/10.1029/2018JB015965

Francou, B., Reynaud, L., 1992. 10 year surficial velocities on a rock glacier (Laurichard, French Alps). Permafrost and Periglacial Processes 3, 209–213. https://doi.org/10.1002/ppp.3430030306

Fu, Z.-F., He, J., 2001. Modal Analysis. Elsevier.

Geo2X, C. de R. sur l'Environnement A. (CREALP), 2014. Reconnaissances géophysiques - Glcair rocheux de Gugla (VS).

Guéguen, P., Langlais, M., Garambois, S., Voisin, C., Douste-Bacqué, I., 2017. How sensitive are site effects and building response to extreme cold temperature? The case of the Grenoble's (France) City Hall building. Bull Earthquake Eng 15, 889–906. https://doi.org/10.1007/s10518-016-9995-3

Guillemot, A., Baillet, L., Helmstetter, A., Larose, É., Mayoraz, R., Garambois, S., under revision. Seismic monitoring of the Gugla rock glacier (Switzerland): observations and modelling. Geophysical Journal International.

Guillemot, A., Helmstetter, A., Larose, É., Baillet, L., Garambois, S., Mayoraz, R., Delaloye, R., 2020. Seismic monitoring in the Gugla rock glacier (Switzerland): ambient noise correlation, microseismicity and modelling. Geophys J Int 221, 1719–1735. https://doi.org/10.1093/gji/ggaa097

Haeberli, W., Hallet, B., Arenson, L., Elconin, R., Humlum, O., Kääb, A., Kaufmann, V., Ladanyi, B., Matsuoka, N., Springman, S., Mühll, D.V., 2006. Permafrost creep and rock glacier dynamics. Permafrost and Periglacial Processes 17, 189–214. https://doi.org/10.1002/ppp.561

Haeberli, W., Noetzli, J., Arenson, L., Delaloye, R., Gärtner-Roer, I., Gruber, S., Isaksen, K., Kneisel, C., Krautblatter, M., Phillips, M., 2010. Mountain permafrost: development and challenges of a young research field. Journal of Glaciology 56, 1043–1058. https://doi.org/10.3189/002214311796406121

Hausmann, H., Krainer, K., Brückl, E., Ullrich, C., 2012. Internal structure, ice content and dynamics of Ölgrube and Kaiserberg rock glaciers (Ötztal Alps, Austria) determined from geophysical surveys. Austrian Journal of Earth Sciences 105(2), 12–31.

Helmstetter, A., Garambois, S., 2010. Seismic monitoring of Séchilienne rockslide (French Alps): Analysis of seismic signals and their correlation with rainfalls. Journal of Geophysical Research: Earth Surface 115. https://doi.org/10.1029/2009JF001532

James, S.R., Knox, H.A., Abbott, R.E., Panning, M.P., Screaton, E.J., 2019. Insights Into Permafrost and Seasonal Active-Layer Dynamics From Ambient Seismic Noise Monitoring. Journal of Geophysical Research: Earth Surface 124, 1798–1816. https://doi.org/10.1029/2019JF005051

Johnson, C.W., Vernon, F., Nakata, N., Ben-Zion, Y., 2019. Atmospheric Processes Modulating Noise in Fairfield Nodal 5 Hz Geophones. Seismological Research Letters 90, 1612–1618. https://doi.org/10.1785/0220180383

Kääb, A., Frauenfelder, R., Roer, I., 2007. On the response of rockglacier creep to surface temperature increase. Global and Planetary Change, Climate Change Impacts on Mountain Glaciers and Permafrost 56, 172–187. https://doi.org/10.1016/j.gloplacha.2006.07.005

Kaufmann, V., Sulzer, W., Seier, G., Wecht, M., 2019. Panta Rhei: Movement Change of Tschadinhorn Rock Glacier (Hohe Tauern Range, Austria), 1954–2017 https://doi.org/10.32909/kg.18.31.1. Kartografija i geoinformacije (Cartography and Geoinformation) 18, 4–24.

Kellerer-Pirklbauer, A., Delaloye, R., Lambiel, C., Gärtner-Roer, I., Kaufmann, V., Scapozza, C., Krainer, K., Staub, B., Thibert, E., Bodin, X., Fischer, A., Hartl, L., di Cella, U.M., Mair, V., Marcer, M., Schoeneich, P., 2018. Interannual variability of rock glacier flow velocities in the European Alps. Presented at the European Conference of Permafrost (EUCOP), Chamonix, France, p. 2.

Kenner, R., Magnusson, J., 2017. Estimating the Effect of Different Influencing Factors on Rock Glacier Development in Two Regions in the Swiss Alps. Permafrost and Periglacial Processes 28, 195–208. https://doi.org/10.1002/ppp.1910

Kenner, R., Pruessner, L., Beutel, J., Limpach, P., Phillips, M., 2019. How rock glacier hydrology, deformation velocities and ground temperatures interact: Examples from the Swiss Alps. Permafrost and Periglacial Processes n/a. https://doi.org/10.1002/ppp.2023

Kneisel, C., Hauck, C., Fortier, R., Moorman, B., 2008. Advances in geophysical methods for permafrost investigations. Permafrost and Periglacial Processes 19, 157–178. https://doi.org/10.1002/ppp.616

Köhler, A., Weidle, C., 2019. Potentials and pitfalls of permafrost active layer monitoring using the HVSR method: a case study in Svalbard. Earth Surface Dynamics 7, 1–16. https://doi.org/10.5194/esurf-7-1-2019

Kula, D., Olszewska, D., Dobiński, W., Glazer, M., 2018. Horizontal-to-vertical spectral ratio variability in the presence of permafrost. Geophys J Int 214, 219–231. https://doi.org/10.1093/gji/ggy118

Kummert, M., Delaloye, R., 2018. Mapping and quantifying sediment transfer between the front of rapidly moving rock glaciers and torrential gullies. Geomorphology 309, 60–76. https://doi.org/10.1016/j.geomorph.2018.02.021

Kummert, M., Delaloye, R., Braillard, L., 2018. Erosion and sediment transfer processes at the front of rapidly moving rock glaciers: Systematic observations with automatic cameras in the western Swiss Alps. Permafrost and Periglacial Processes 29, 21–33. https://doi.org/10.1002/ppp.1960

Lacroix, P., Helmstetter, A., 2011. Location of Seismic Signals Associated with Microearthquakes and Rockfalls on the Sechilienne Landslide, French Alps. Bulletin of The Seismological Society of America - BULL SEISMOL SOC AMER 101. https://doi.org/10.1785/0120100110

Larose, E., Carrière, S., Voisin, C., Bottelin, P., Baillet, L., Guéguen, P., Walter, F., Jongmans, D., Guillier, B., Garambois, S., Gimbert, F., Massey, C., 2015. Environmental seismology: What can we learn on earth surface processes with ambient noise? Journal of Applied Geophysics 116, 62–74. https://doi.org/10.1016/j.jappgeo.2015.02.001

Leclaire, Ph., Cohen-Ténoudji, F., Aguirre-Puente, J., 1994. Extension of Biot's theory of wave propagation to frozen porous media. The Journal of the Acoustical Society of America 96, 3753–3768. https://doi.org/10.1121/1.411336

Lévy, C., Baillet, L., Jongmans, D., Mourot, P., Hantz, D., 2010. Dynamic response of the Chamousset rock column (Western Alps, France). Journal of Geophysical Research: Earth Surface 115. https://doi.org/10.1029/2009JF001606

Marcer, M., Nielsen, S., Ribeyre, C., Kummert, M., Duvillard, P.A., Bodin, X., Schoeneich, P., Génuite, K., 2019a. Investigating the slope failures at the Lou rock glacier front, French Alps. Permafrost and Periglacial Processes.

Marcer, M., Serrano, C., Brenning, A., Bodin, X., Goetz, J., Schoeneich, P., 2019b. Evaluating the destabilization susceptibility of active rock glaciers in the French Alps. The Cryosphere 13, 141–155. https://doi.org/10.5194/tc-13-141-2019

Marsy, G., Vernier, F., Bodin, X., Castaings, W., Trouvé, E., 2018. Détection automatique de zones en mouvement dans des séries d'images non recalées: application à la surveillance des mouvements gravitaires. Revue Française de Photogrammétrie et de Télédétection 25–31.

Maurer, H., Hauck, C., 2007. Geophysical imaging of alpine rock glaciers. Journal of Glaciology 53, 110–120. https://doi.org/10.3189/172756507781833893

Merz, K., Maurer, H., Rabenstein, L., Buchli, T., Springman, S.M., Zweifel, M., 2016. Multidisciplinary geophysical investigations over an alpine rock glacierMultigeophysics over a rock glacier. Geophysics 81, WA1–WA11. https://doi.org/10.1190/geo2015-0157.1

Michel, C., Guéguen, P., Arem, S.E., Mazars, J., Kotronis, P., 2010. Full-scale dynamic response of an RC building under weak seismic motions using earthquake recordings, ambient vibrations and modelling. Earthquake Engineering & Structural Dynamics 39, 419–441. https://doi.org/10.1002/eqe.948

Michel, C., Guéguen, P., Bard, P.-Y., 2008. Dynamic parameters of structures extracted from ambient vibration measurements: An aid for the seismic vulnerability assessment of existing buildings in moderate seismic hazard regions. Soil Dynamics and Earthquake Engineering 28, 593–604. https://doi.org/10.1016/j.soildyn.2007.10.002

Mordret, A., Mikesell, T.D., Harig, C., Lipovsky, B.P., Prieto, G.A., 2016. Monitoring southwest Greenland's ice sheet melt with ambient seismic noise. Science Advances 2, e1501538. https://doi.org/10.1126/sciadv.1501538

Parolai, S., 2002. New Relationships between Vs, Thickness of Sediments, and Resonance Frequency Calculated by the H/V Ratio of Seismic Noise for the Cologne Area (Germany). Bulletin of the Seismological Society of America 92, 2521–2527. https://doi.org/10.1785/0120010248

Preiswerk, L.E., Michel, C., Walter, F., Fäh, D., 2019. Effects of geometry on the seismic wavefield of Alpine glaciers. Annals of Glaciology 60, 112–124. https://doi.org/10.1017/aog.2018.27

Preiswerk, L.E., Walter, F., 2018. High-Frequency (>2 Hz) Ambient Seismic Noise on High-Melt Glaciers: Green's Function Estimation and Source Characterization. Journal of Geophysical Research: Earth Surface 123, 1667–1681. https://doi.org/10.1029/2017JF004498

RESIF, 1995. RESIF-RLBP French Broad-band network, RESIF-RAP strong motion network and other seismic stations in metropolitan France [Data set]. RESIF - Réseau Sismologique et géodésique Français. https://doi.org/10.15778/RESIF.FR.

Rice, R.W., 1993. Evaluating Porosity Parameters for Porosity-Property Relations. J American Ceramic Society 76, 1801–1808. https://doi.org/10.1111/j.1151-2916.1993.tb06650.x

Roeoesli, C., Walter, F., Ampuero, J.-P., Kissling, E., 2016. Seismic moulin tremor. Journal of Geophysical Research: Solid Earth 121, 5838–5858. https://doi.org/10.1002/2015JB012786

Roux, P., Guéguen, P., Baillet, L., Hamze, A., 2014. Structural-change localization and monitoring through a perturbation-based inverse problem. The Journal of the Acoustical Society of America 136, 2586–2597. https://doi.org/10.1121/1.4897403

Scotti, R., Crosta, G.B., Villa, A., 2017. Destabilisation of Creeping Permafrost: The Plator Rock Glacier Case Study (Central Italian Alps). Permafrost and Periglacial Processes 28, 224–236. https://doi.org/10.1002/ppp.1917

Snieder, R., Larose, E., 2013. Extracting Earth's Elastic Wave Response from Noise Measurements. Annual Review of Earth and Planetary Sciences 41, 183–206. https://doi.org/10.1146/annurev-earth-050212-123936

Solomon, J., 1991. PSD computations using Welch's method. [Power Spectral Density (PSD)] (No. SAND-91-1533). Sandia National Labs., Albuquerque, NM (United States). https://doi.org/10.2172/5688766

Spillmann, T., Maurer, H., Green, A.G., Heincke, B., Willenberg, H., Husen, S., 2007. Microseismic investigation of an unstable mountain slope in the Swiss Alps. Journal of Geophysical Research: Solid Earth 112. https://doi.org/10.1029/2006JB004723

Springman, S.M., Yamamoto, Y., Buchli, T., Hertrich, M., Maurer, H., Merz, K., Gärtner-Roer, I., Seward, L., 2013. Rock Glacier Degradation and Instabilities in the European Alps: A Characterisation and Monitoring Experiment in the Turtmanntal, CH, in: Margottini, C., Canuti, P., Sassa, K. (Eds.), Landslide Science and Practice: Volume 4: Global Environmental Change. Springer, Berlin, Heidelberg, pp. 5–13. https://doi.org/10.1007/978-3-642-31337-0_1

Strozzi, T., Caduff, R., Jones, N., Barboux, C., Bodin, X., Kääb, A., Mätzler, E., Schrott, L., 2020. Monitoring Rock Glacier Kinematics with Satellite Synthetic Aperture Radar. Remote Sensing 25.

Timur, A., 1968. Velocity of compressional waves in porous media at permafrost temperatures. GEOPHYSICS 33, 584–595. https://doi.org/10.1190/1.1439954

Wathelet, M., Jongmans, D., Ohrnberger, M., 2004. Surface-wave inversion using a direct search algorithm and its application to ambient vibration measurements. Near Surface Geophysics 2, 211–221. https://doi.org/10.3997/1873-0604.2004018

Weber, S., Fäh, D., Beutel, J., Faillettaz, J., Gruber, S., Vieli, A., 2018. Ambient seismic vibrations in steep bedrock permafrost used to infer variations of ice-fill in fractures. Earth and Planetary Science Letters 501, 119–127. https://doi.org/10.1016/j.epsl.2018.08.042

Weber, Samuel, Faillettaz, J., Meyer, M., Beutel, J., Vieli, A., 2018. Acoustic and Microseismic Characterization in Steep Bedrock Permafrost on Matterhorn (CH). Journal of Geophysical Research: Earth Surface 123, 1363–1385. https://doi.org/10.1029/2018JF004615

Wirz, V., Gruber, S., Purves, R.S., Beutel, J., Gärtner-Roer, I., Gubler, S., Vieli, A., 2016. Short-term velocity variations at three rock glaciers and their relationship with meteorological conditions. Earth Surface Dynamics 4, 103–123. https://doi.org/10.3929/ethz-b-000114470

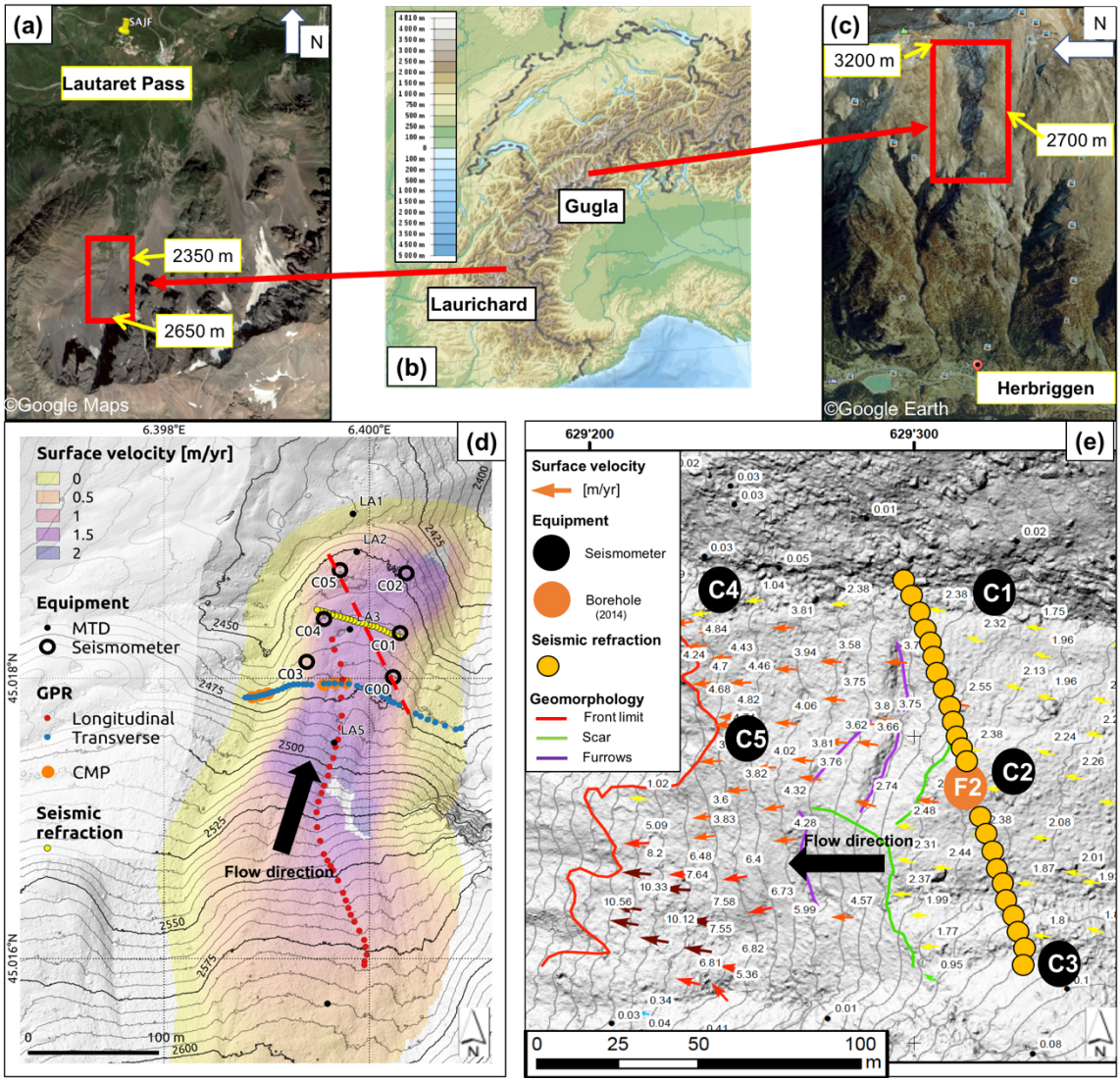

Figure 1: (a,c) Aerial views of the two sites (from ©Google Maps and ©Google Earth). (b) Global topographic map of the western part of the alpine belt, centered around the French and Swiss Alps. (d) Digital elevation model of the Laurichard rock glacier, and location of the Miniature Temperature Dataloggers (MTD) that monitor ground thermal regime at the sub-surface, the seismometers, and the geophysical surveys: Ground Penetrating Radar (GPR, red and blue points); seismic refraction profile (yellow points). The mean annual surface velocity fields (over the period 2012-2017) is revealed by the background color. The 6 continuous seismometers are marked by large circles (C00 to C05). The dashed red line depicts the C00-C05 profile used for the bedrock depth estimation (see Figure 8). (e) Digital elevation model of the Gugla rock glacier (front in red line) and location of instrumentation, the seismic refraction profile and geomorphologic features. The mean annual surface velocity measured between 2014 and 2015 by photogrammetry (CREALP, 2016) is also shown on this map.

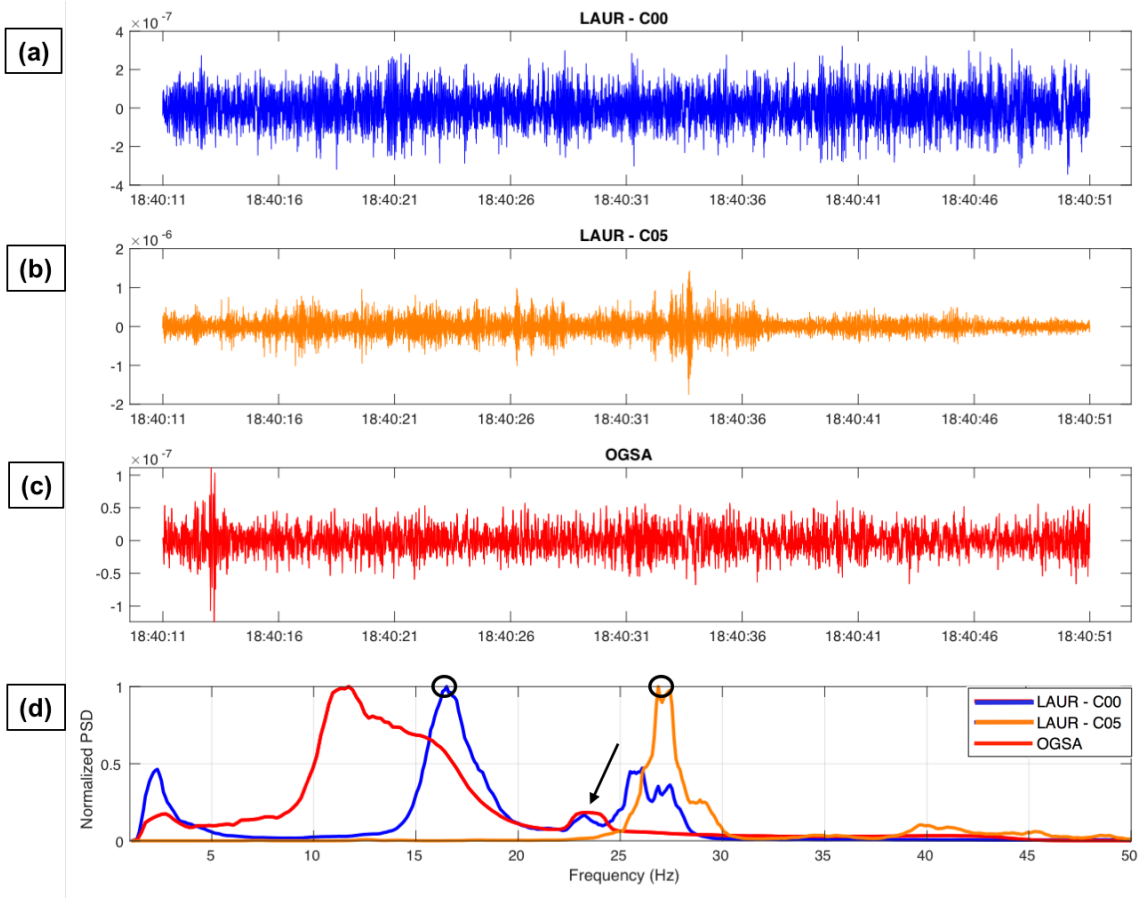

Figure 2: Seismic recordings of ambient noise (vertical ground velocity in m/s, after >1Hz filtering and instrumental deconvolution) recorded by sensors C00 (a) and C05 (b) in Laurichard rock glacier, and by OGSA station at Lautaret pass (c), the 5th April 2019 at 6 PM. (d) The normalized PSD of the respective signals. Black circles highlight the maxima of these spectrograms that have been picked by using our method (details in the text) for sensors on Laurichard rock glacier. The black arrow shows the stable peak at 23 Hz, interpreted as anthropogenic, measured by all sensors (but not clear for C05 sensor due to normalization).

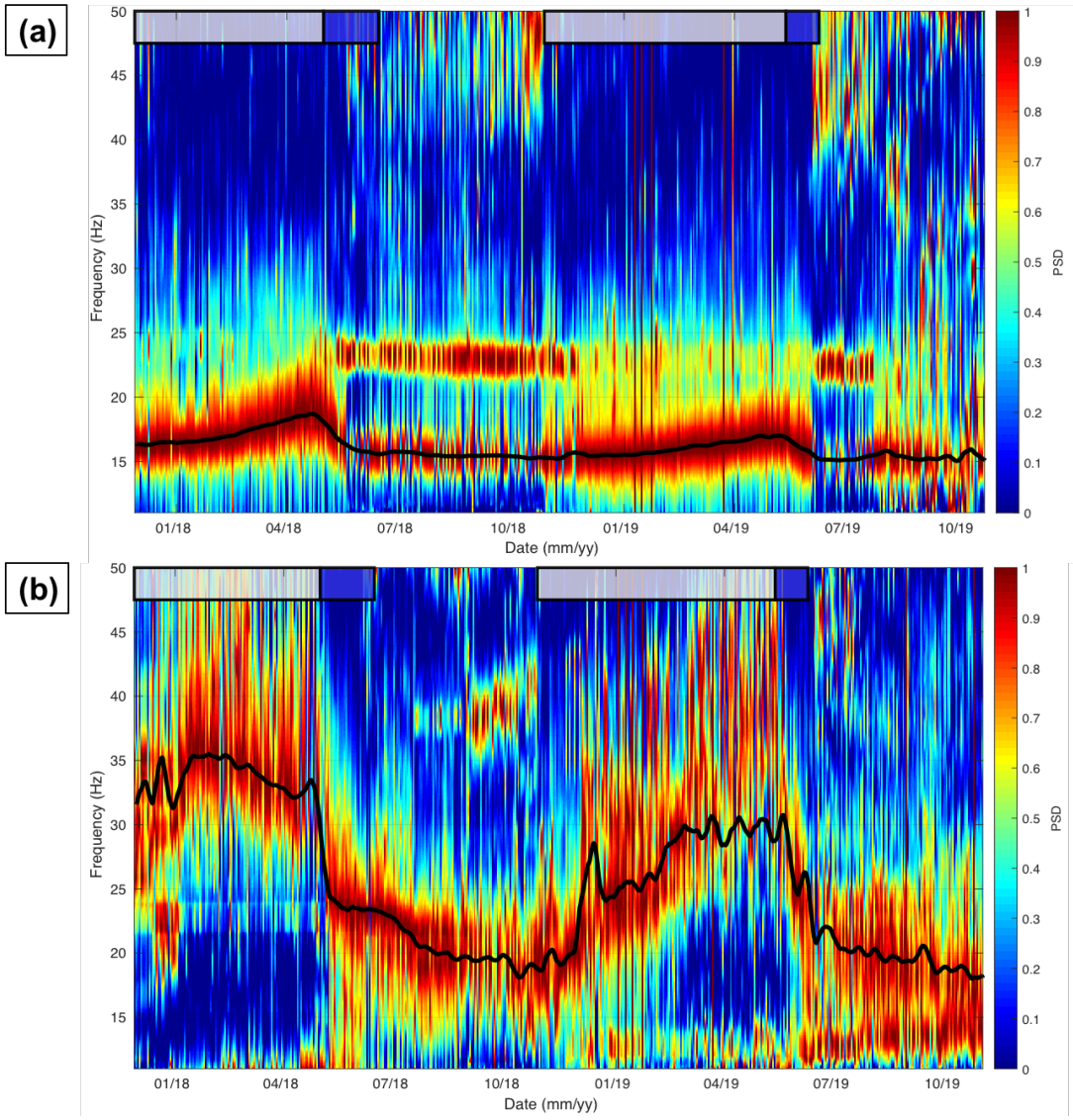

Figure 3: Normalized Power Spectra Density (PSD) from hourly spectrograms of the passive seismic recordings of Laurichard site, respectively from (a) C00 seismometer and from (b) C05 seismometer. The bold black line denotes the moving window average of hourly spectrogram maxima. Snow cover and melting periods are both figured by grey and blue boxes above, respectively.

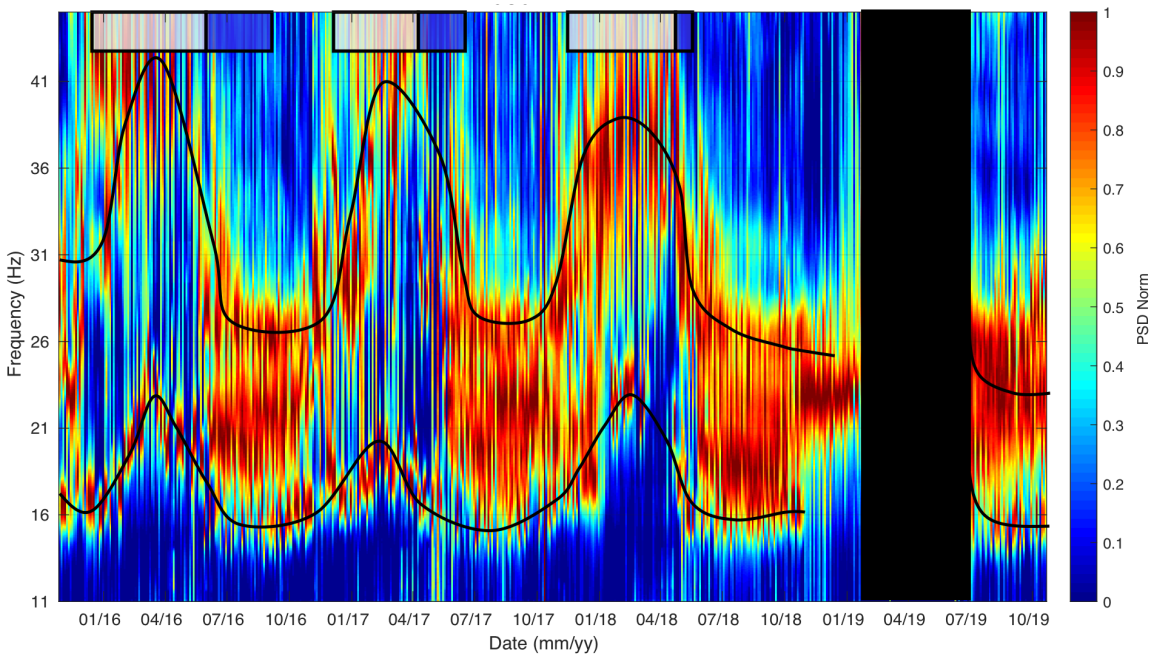

Figure 4 : Normalized Power Spectral Density (PSD) from hourly spectrograms of the ambient noise recordings of Gugla rock glacier, from C2 seismometer. Note the two bold black lines that roughly highlight the two picked spectral modes, for visibility purposes. Snow cover and melting periods are both figured by grey and blue boxes above, respectively. No-data period is marked by a black box.

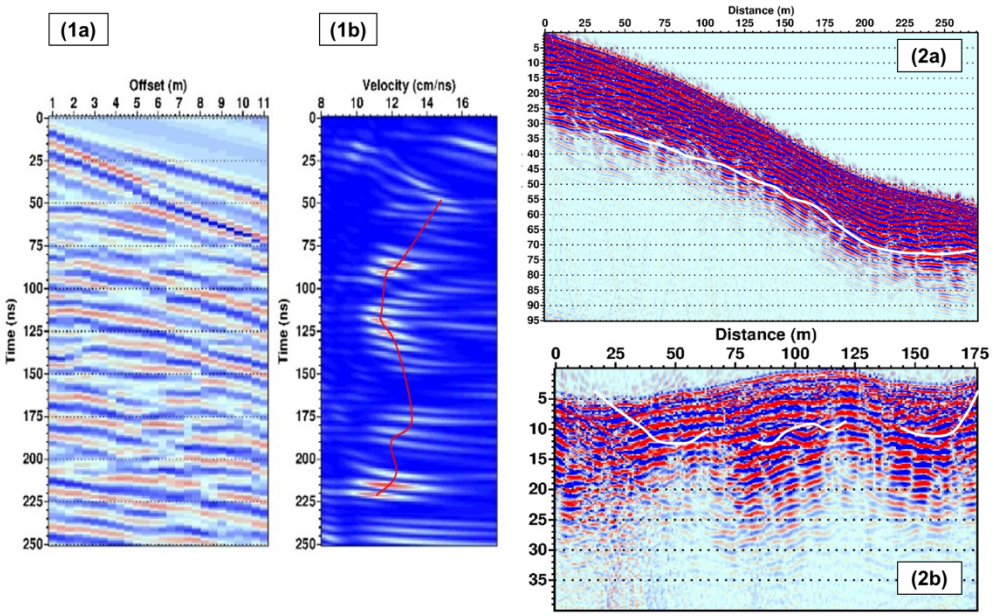

Figure 5: GPR results for Laurichard rock glacier, with: (1a) Common Middle Point GPR data acquired with a 100 MHz unshielded antenna. (1b) velocity analysis displaying the semblance according to apparent velocity and propagation time. The red curve indicates the picked maximum of semblance. (2) Common-offset 25 MHz profiles : (a) Longitudinal profile. Elevation corrections have been divided by a factor of 2 for visibility purposes. (b) Transverse profile. On both cases, the vertical/horizontal ratio axis has been scaled by a factor of 2.4, and the bedrock interface is highlighted by a white curve.

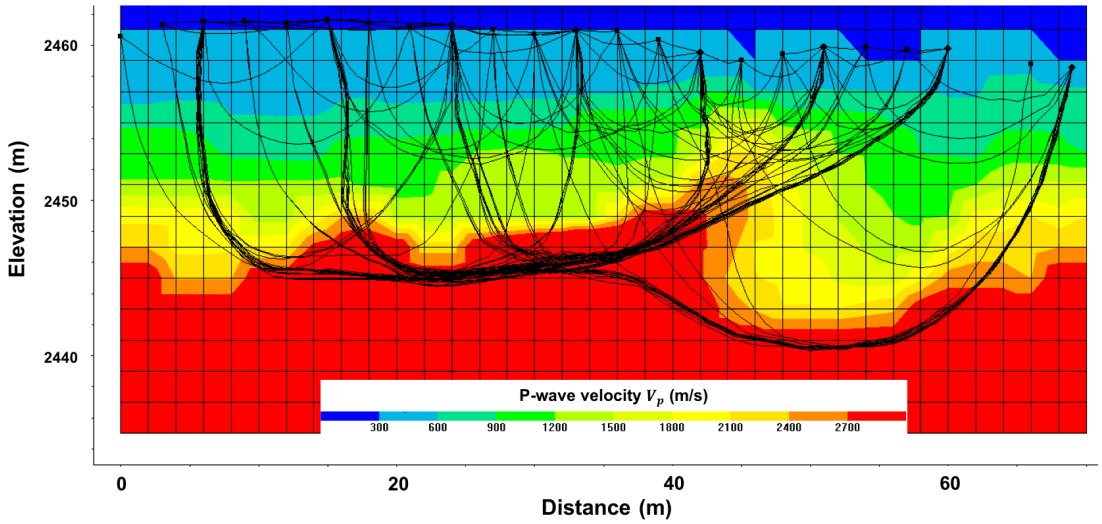

Figure 6: P-wave velocity distribution obtained from a seismic tomography acquired along the transversal profile of seismic refraction (yellow line in Fig. 1a) in summertime. The different ray paths are shown with black curves. The seismic velocities were used to constrain bedrock depth and P-wave velocity profiles for the mechanical modeling.

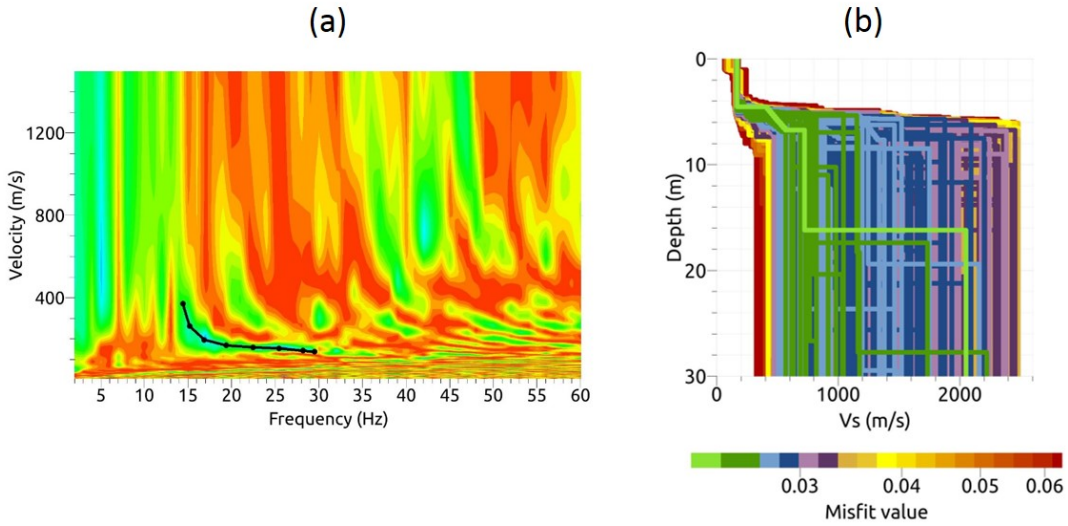

Figure 7: Multichannel analysis of Rayleigh waves propagating within the rock glacier. (a) semblance velocity-frequency map highlighting several modes, the fundamental dispersion curve being picked as indicated by the black line and (b) Vs distribution versus depth derived from the inversion of the fundamental dispersion curve. Colors indicate the RMS error (colorbar in %) between synthetic and picked fundamendal dispersion curves (best fitting model in green).

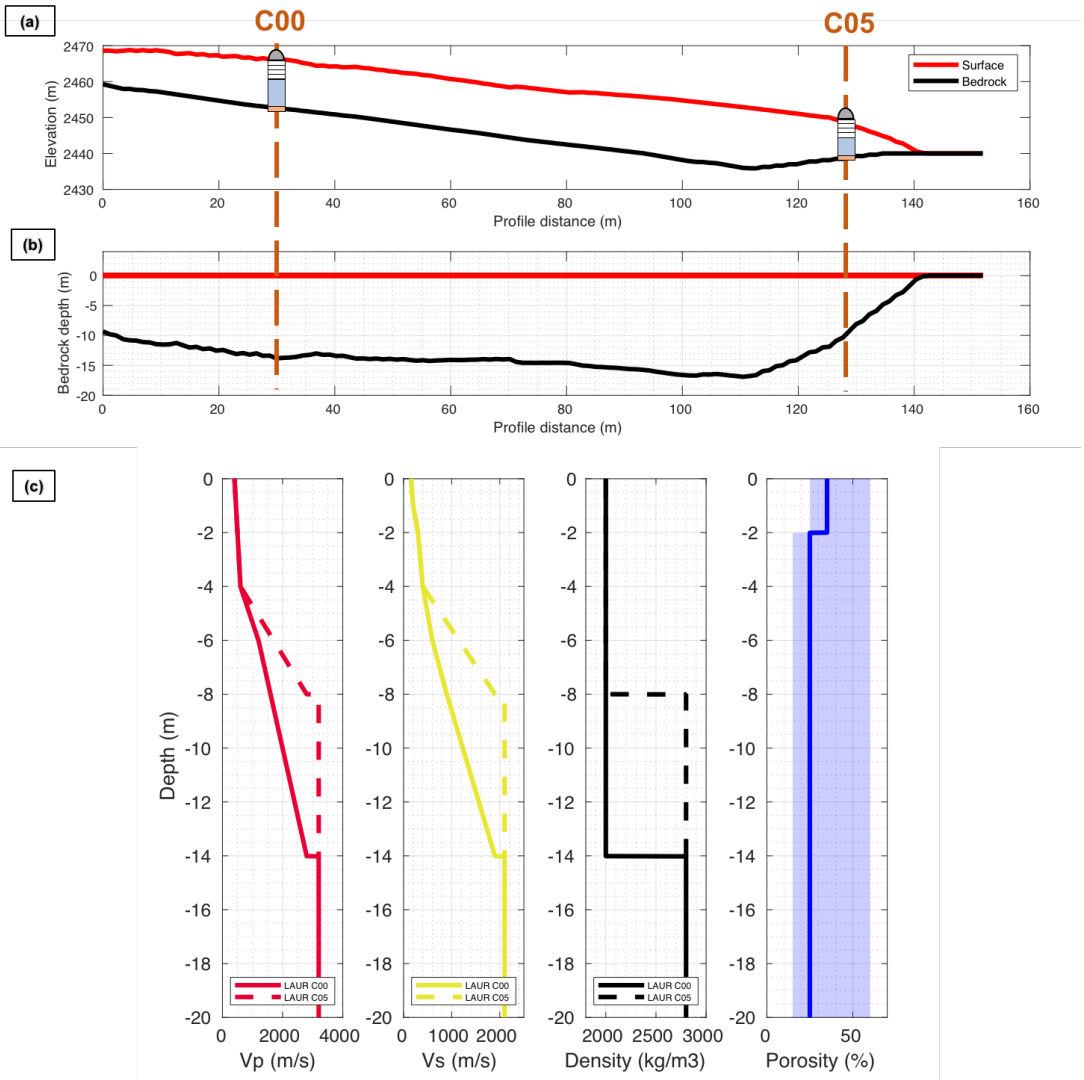

Figure 8 : (a) Cross-section of the Laurichard rock glacier Digital Elevation Models (DEM) of the surface and of the bed (taken for the bedrock) along the C05-C00 line. (b) The same profile, with the DEM of the surface as the reference. The vertical axis is then the bedrock depth starting from the surface. For both figures the location of the seismometers is indicated. (c) Seismic velocity models of the Laurichard rock glacier (continuous line for the C00 case, dashed line for the C05 case), based on geophysical investigations (seismic refraction) and the bedrock depth estimation, determined from DEM difference (see 1b). The only difference between the two cases is the bedrock depth, and consequently the seismic velocity gradient of the

permafrost layer. On right panels the density and the medium porosity profile are shown (solid blue curve), with low and high limits of the porosity used in the following mechanical modelling.

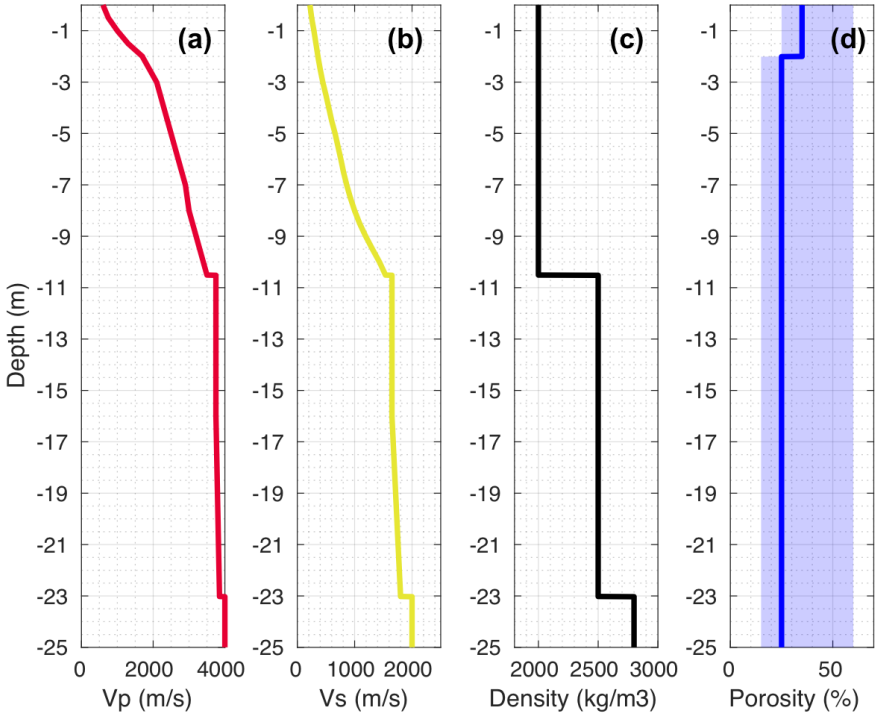

Figure 9 : Seismic velocity models of the Gugla rock glacier, based on geophysical investigations (seismic refraction) and from borehole data, with P-wave velocity (a) and S-wave velocity (b) profiles. The density (c) and the medium porosity ((d), solid blue curve) profiles are also shown, with low and high limits of the porosity used in the following mechanical modelling.

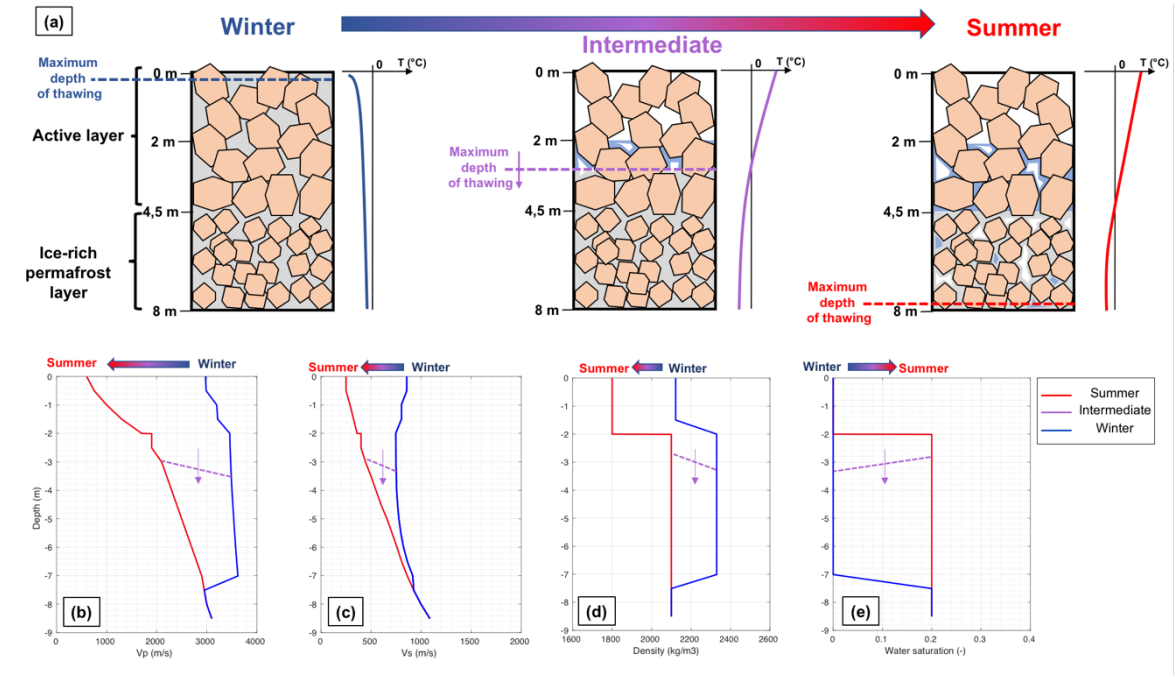

885 Figure 10: (a) Schematic cross-section of the Gugla rock glacier in winter (left) and in summer (right), and during the transition between them (intermediate state of thawing, in middle), as well as a schematic temperature profile associed with each of them, showing the main assumptions of the freezing modeling methodology by a poroelastic approach described in the text. The porous medium is composed of a rock matrix (in orange) and pores filled by water (in blue) or ice (in grey). With respect to the maximum depth of thawing varying from the surface to the ZAA depth, the evolution of parameters used by the model is
890 respectively showed : P-wave velocity (b), S-wave velocity (c), the averaged density (d) and the water saturation (d). The values in summer are obtained from geophysics and boreholes, whereas the values corresponding to a frozen state (pores fully filled by ice, no more liquid water) are obtained by the 3-phases poroelastic model.

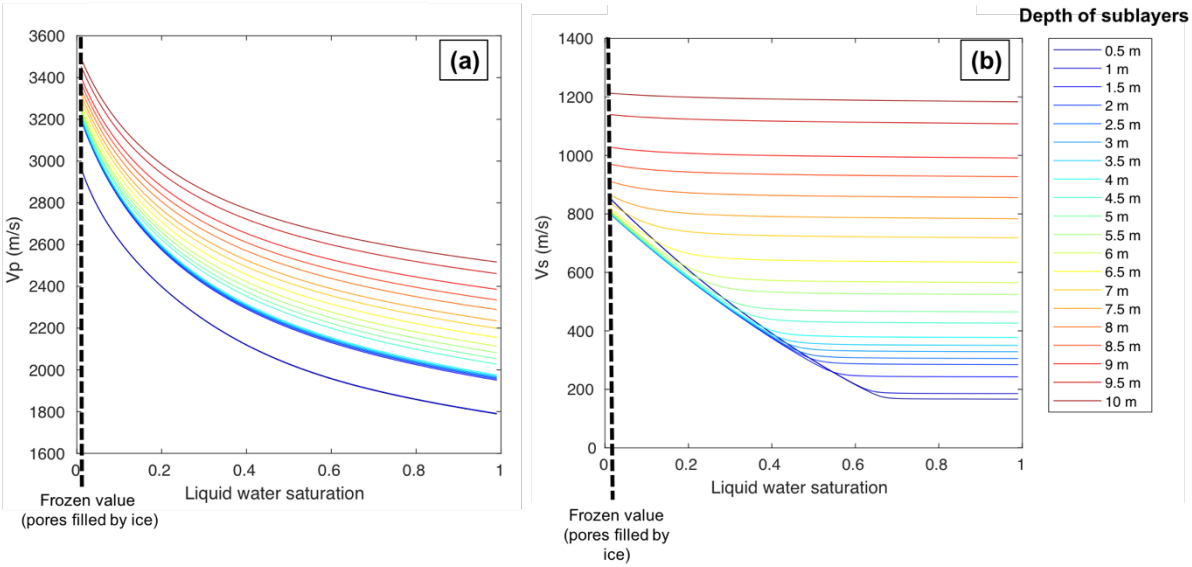

Figure 11: (a) Evolution of P-wave velocity V_p with respect to the ratio between water and ice filling the pores, resulting from the Biot-Gassmann type three-phase poroelastic model, applied to the Laurichard rock glacier (for C00 seismometer). The different curves correspond to the different sublayers, whose depth is indicated in the right panel. The V_p values used to model the winter state are those for liquid water saturation tending towards zero. (b) Same results for S-wave velocity V_s.

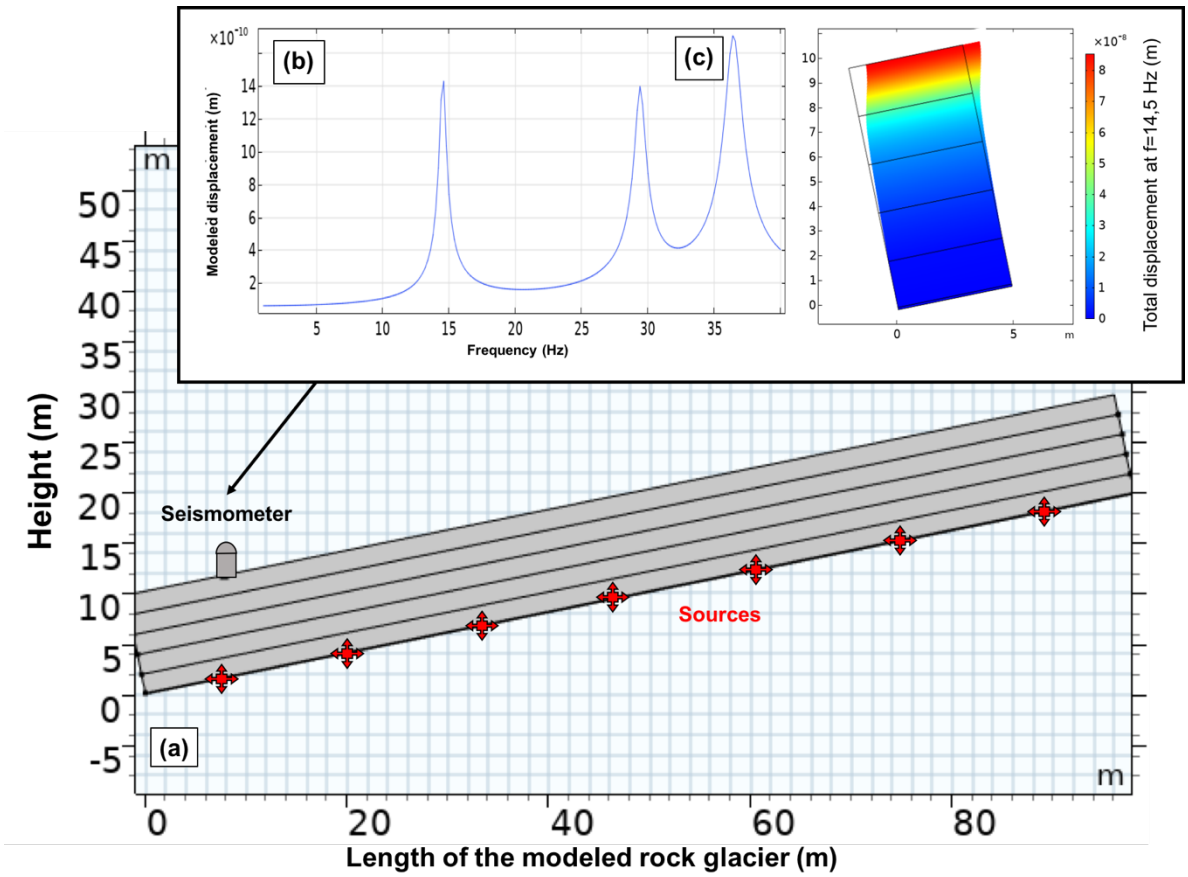

Figure 12: (a) First 2-D model of the terminal part of Laurichard rock glacier, with realistic longitudinal dimension (length) and location of synthetic seismic sources and seismometer. (b) Output of the Frequency Response Function (FRF) of this model, as the vertical displacement recorded by the seismometer along frequencies. Peaks of this curve indicates resonance frequencies of modes of the modeled structure with a vertical component. (c) The 2-D rock glacier model with reduced longitudinal dimension (5 m), and with symmetrical conditions at boundaries perpendicular to the slope. Since the FRF of this model shows the same peaks than the first one, this reduced model is only used for the modal analysis for the sake of simplicity.

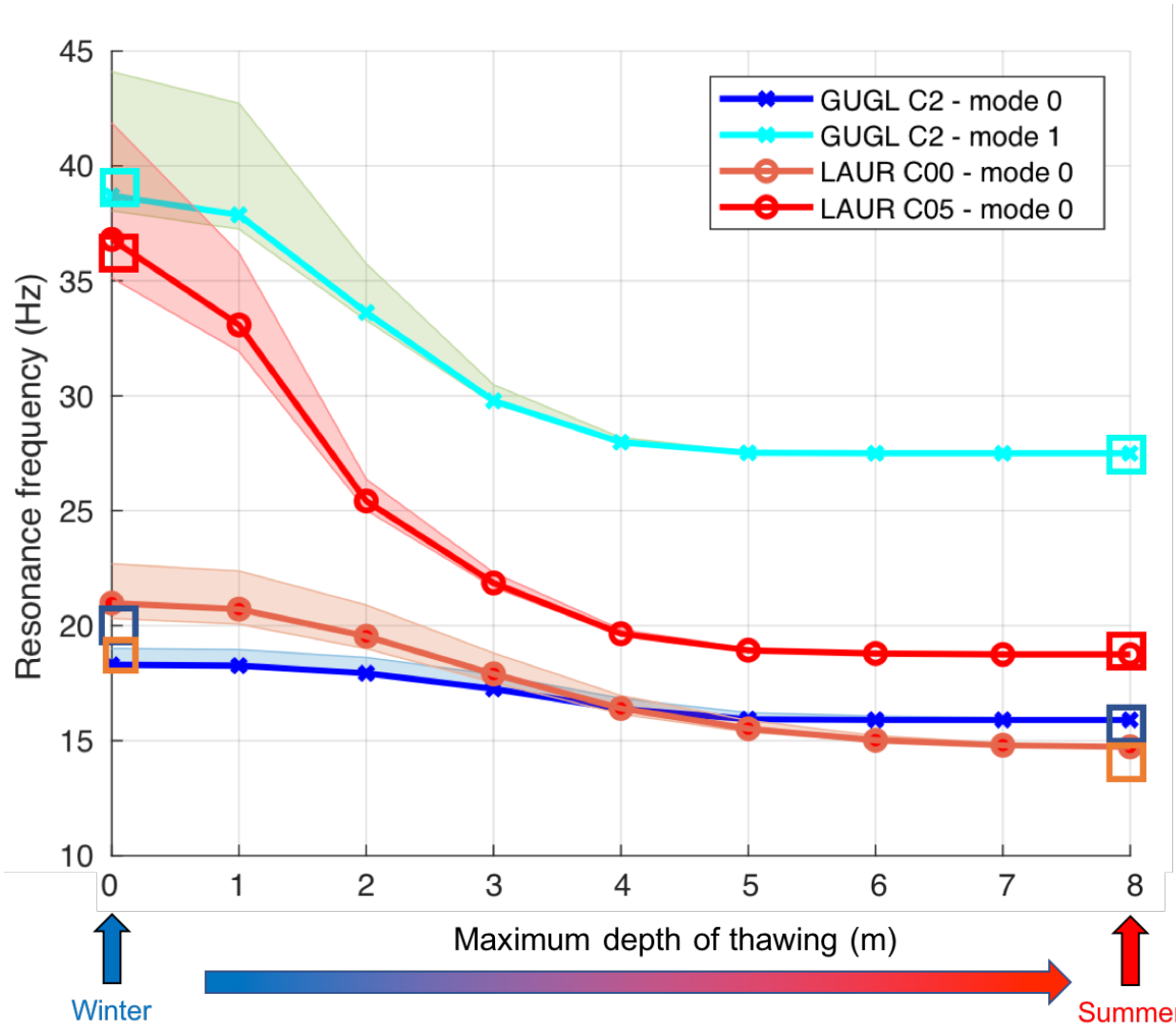

Figure 13: Results of the modal analysis for Gugla (GUGL) and Laurichard (LAUR) rock glaciers. The evolution of the resonance frequency of the respective synthetic modes is plotted, according to the maximal depth of thawing from the surface to the ZAA (8 m depth): left stands for the state of maximal freezing in winter (frozen medium until 8 m depth), right for the summer (unfrozen medium). The range of measured resonance frequency values is shown by the squares in the corresponding colors (estimated from Figure 3 and Figure 4 for respective sites). Errorbars (in transparence) show the influence of porosity on the results : the low (high) limit of errorbars shows the results for extremely low (extremely high) porosity profile.

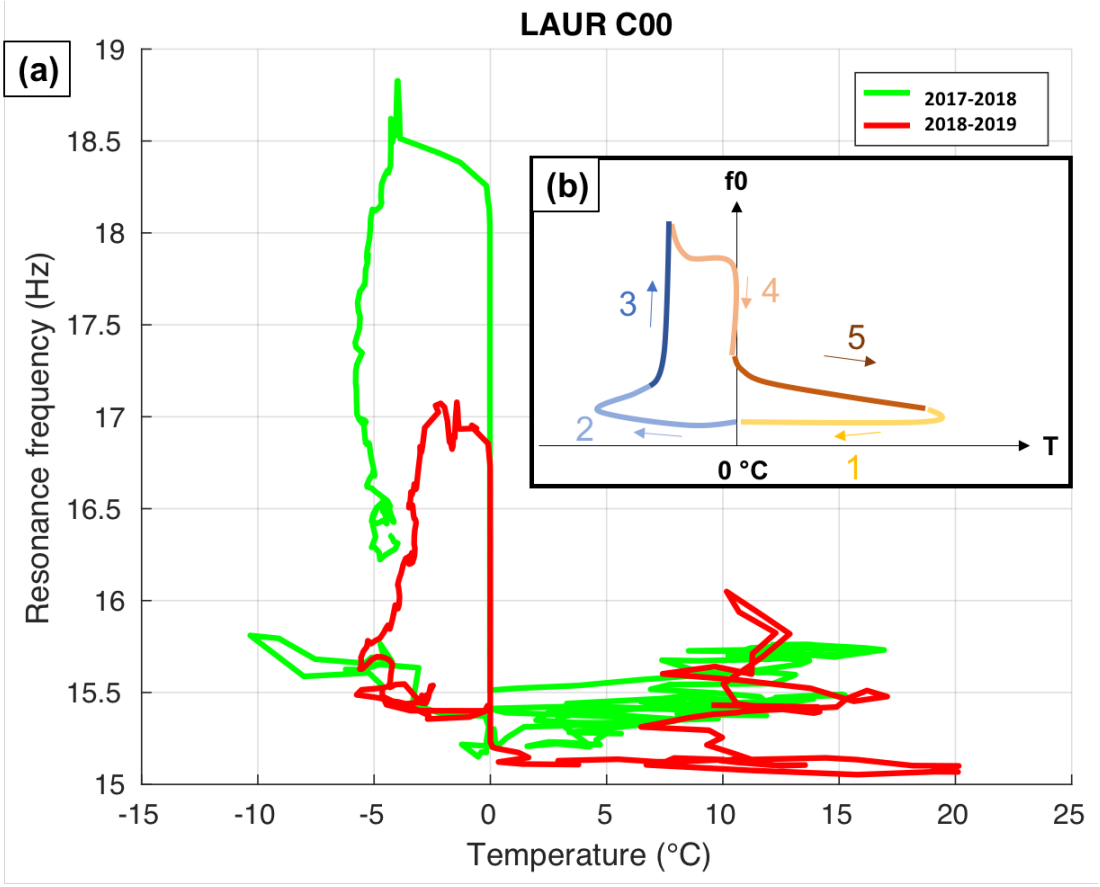

Figure 14: (a) Diagram of daily-averaged ground temperature (recorded by Miniature Temperature Dataloggers) versus daily-averaged resonance frequency of the first mode recorded by C00 seismometer at Laurichard rock glacier. The green curve corresponds to data from December 2017 to November 2018, while the red curve corresponds to data from December 2018 to October 2019. (b) Schematic generalization of the ground surface temperature dependency of resonance frequency with freezing-thawing cycle, showing an hysteretic loop composed of five phases described in the text.

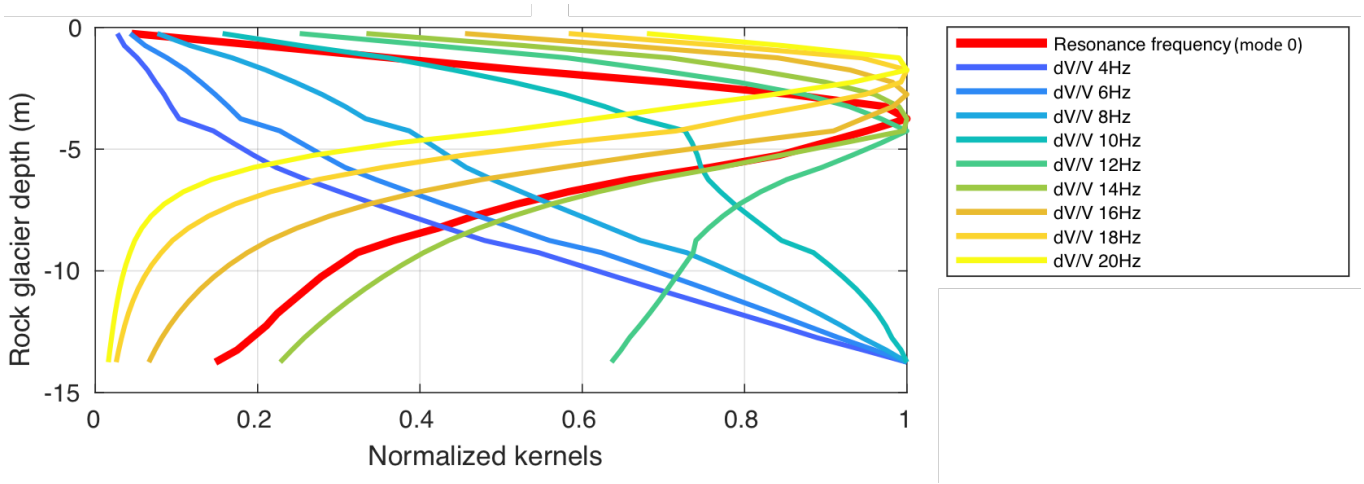

Figure 15 : Example of (normalized) depth sensitivity kernels of the two passive seismic methods for the Laurichard (C00 seismometer) rock glacier model. The red curve corresponds to the modal analysis (resonance frequency of the first vibrating mode). The other curves correspond to the ambient noise correlation (relative change of the Rayleigh wave velocity dV/V, depending of the frequency, shown by the other colours). At high frequencies (> 14Hz), dV/V is most sensitive at shallower depths than the resonance frequency of the first mode, whereas at low frequencies (< 14Hz), dV/V is most sensitive at deeper depths than resonance frequency.

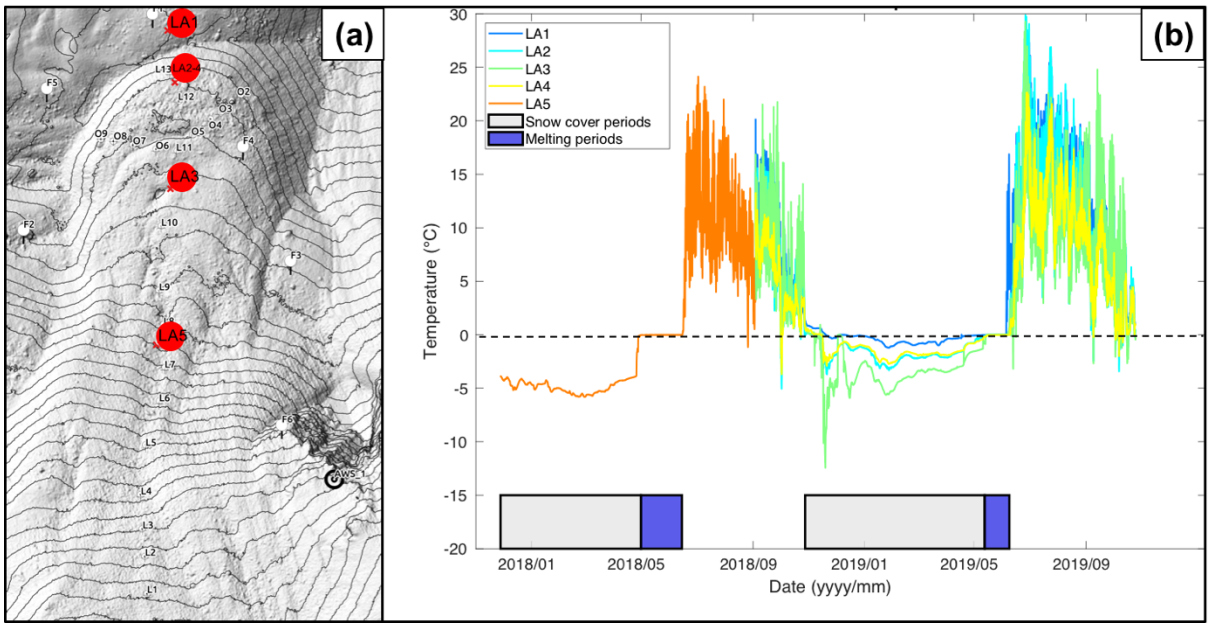

Figure 16 : (a) Location of the five Miniature Temperature Dataloggers (MTD) that record every hour the temperature of the sub-surface (below 2-10 cm of debris), shown in (b) over the two first years of data, with highlighting snow cover (grey boxes, when temperature is below 0°C) and melting periods (blue boxes, when zero-curtain effect occurs).

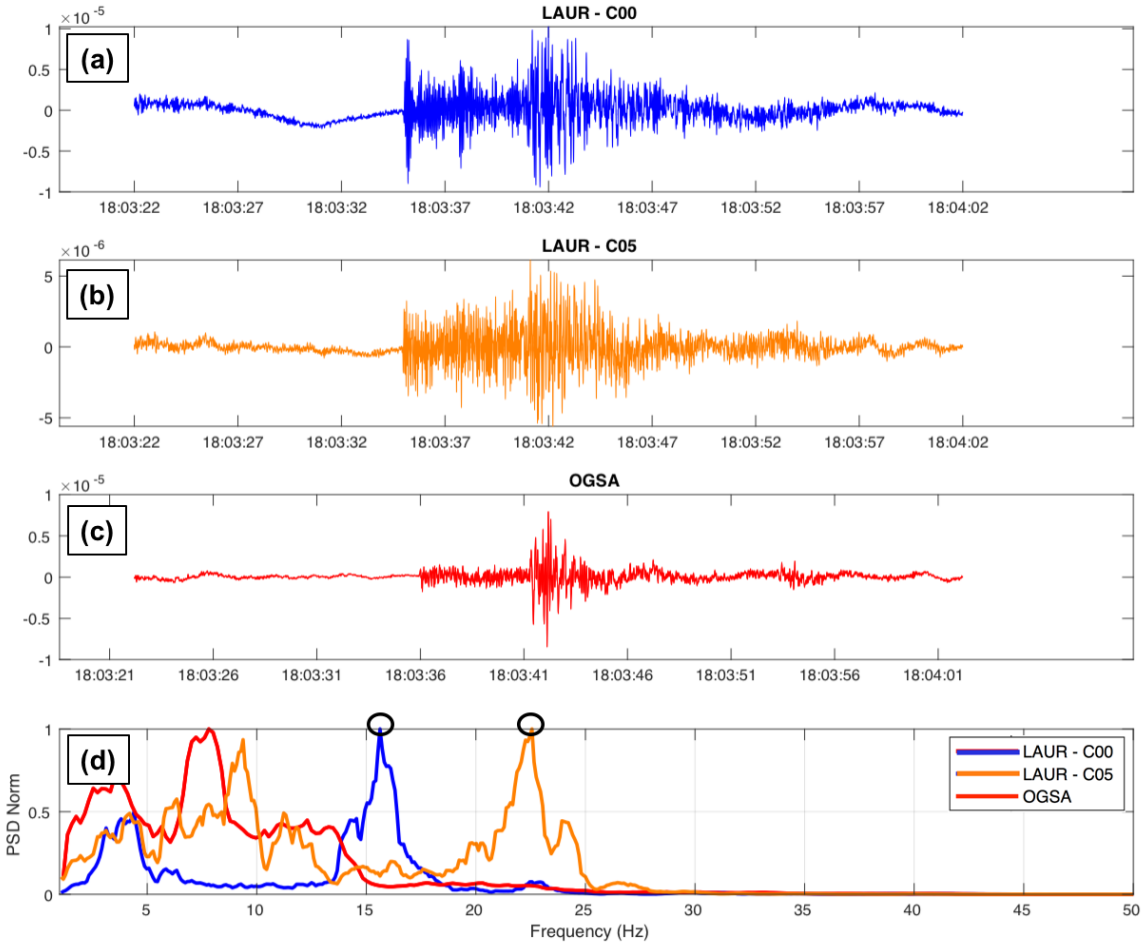

Figure 17: Seismic signals of an earthquake (vertical ground velocity in m/s) recorded by sensors C00 (a) and C05 (b) in Laurichard rock glacier, and by OGSA station at Lautaret pass (c), the 29rd June 2018 at 6 PM. (d) The normalized PSD of the respective signals. Black circles highlight the maxima of these spectrograms that have been picked by using our method (details in the text). The same method has been used for ambient noise recordings.

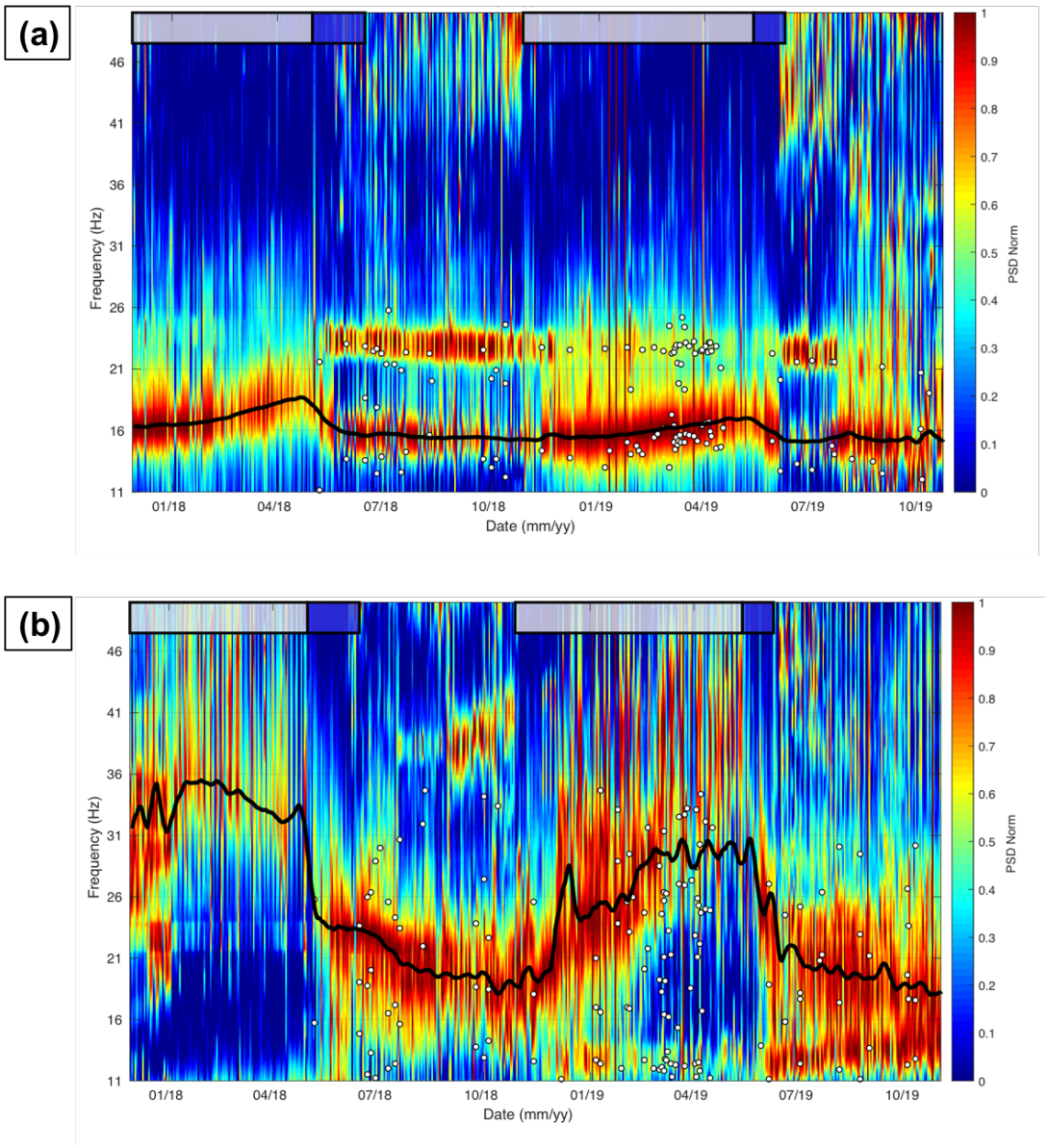

Figure 18: Normalized Power Spectra Density (PSD) from hourly spectrograms of the passive seismic recordings of Laurichard site, respectively from (a) C00 seismometer and from (b) C05 seismometer. The bold black line denotes the moving window average of hourly spectrogram maxima. For each recorded earthquake (M>2), the local maxima have been automatically picked (white dots) if it appears significantly on the spectrogram. Snow cover and melting periods are both figured by white and blue boxes above, respectively.

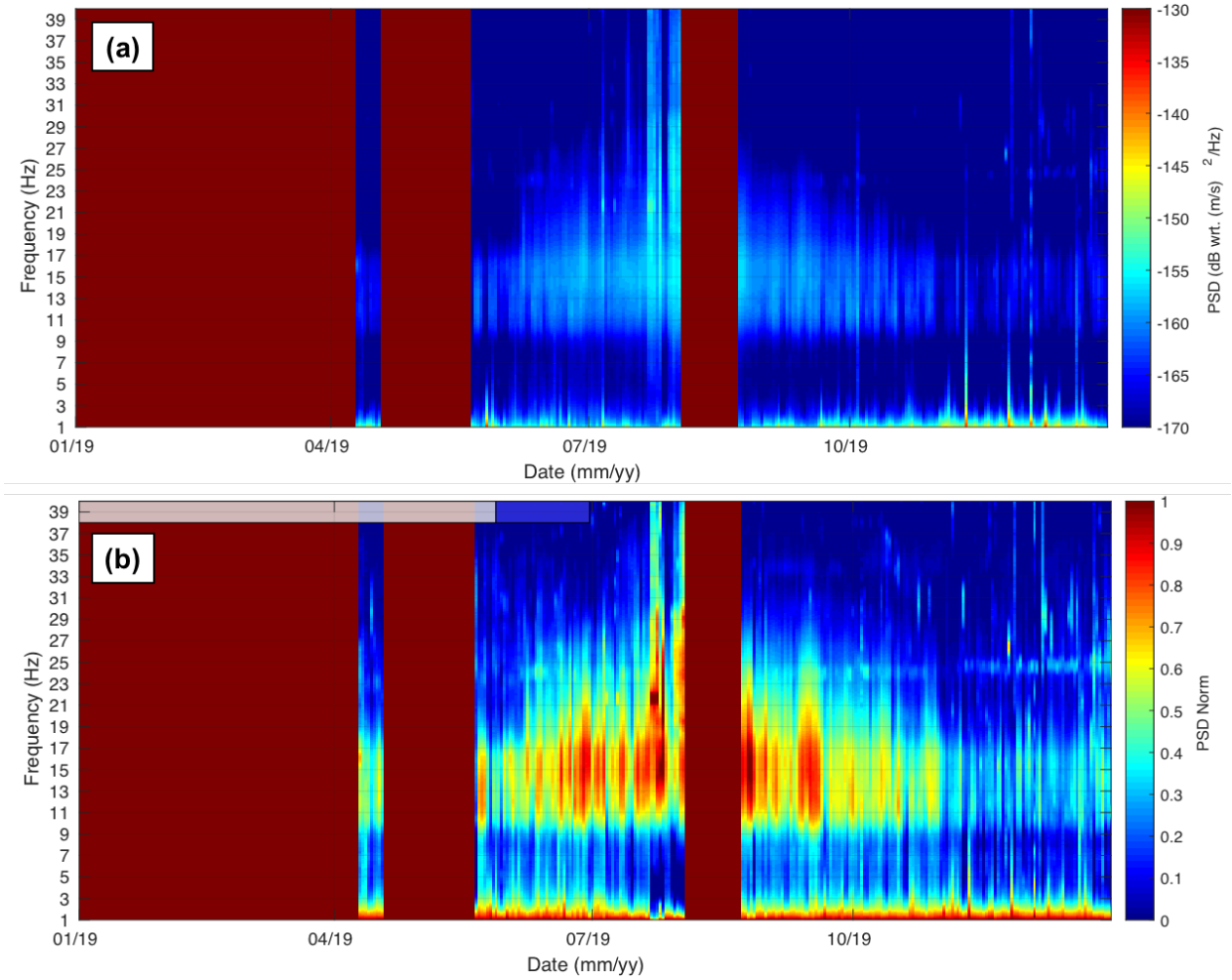

Figure 19 : Daily raw (a) and normalized (b) spectrograms of Power Spectral Density (PSD) from OGSA station, located at 2 km from the Laurichard rock glacier, in a stable site, for all the year 2019.